Published in final edited form as:

Health Phys. 2020 November ; 119(5): 559–587. doi:10.1097/HP.0000000000001346.

Acute radiation-induced lung injury in the nonhuman primate: a review and comparison of mortality and co-morbidities using models of partial-body irradiation with marginal bone marrow sparing and whole thorax lung irradiation

Thomas J. MacVittie[1], **Ann M. Farese**[1], **George A. Parker**[2], **Alexander W. Bennett**[3], **William Jackson III**[4]

[1]University of Maryland School of Medicine, Baltimore, MD

[2]Charles River Laboratories, Durham, NC

[3]Louisville, KY, formerly at University of Maryland School of Medicine, Baltimore, MD

[4]Rockville, MD

Abstract

Purpose: The nonhuman primate, rhesus macaque, is a relevant animal model that has been used to determine the efficacy of medical countermeasures to mitigate major signs of morbidity and mortality of radiation-induced lung injury. Herein a literature review of published studies showing the evolution of lethal lung injury characteristic of the delayed effects of acute radiation exposure between the two significantly different exposure protocols, whole thorax lung irradiation and partial-body irradiation with bone marrow sparing in the nonhuman primate is provided.

Methods: The selection of published data was made from the open literature. The primary studies conducted at two research sites benefitted from the similarity of major variables, namely, both sites used rhesus macaques of approximate age and body weight; radiation exposure by LINAC-derived 6 MV photons at dose rates of 0.80 Gy min^{-1} and 1.00 Gy min^{-1} delivered to the midline tissue via bilateral, anterior/posterior, posterior/anterior geometry. An advantage relative to sex difference, resulted from the use male and female macaques by the Maryland and the Washington sites, respectively. Subject-based medical management was used for all macaques.

Results: The primary studies (6) provided adequate data to establish dose response relationships within 180 d for the radiation-induced lung injury consequent to whole thorax lung irradiation (male vs female) and partial-body irradiation with bone marrow sparing exposure protocols (male). The dose response relationships established by probit analyses versus linear dose relationships were characterized by two main parameters or dependent variables, a slope and LD50/180. Respective LD50/180 values for the primary studies that used whole thorax lung irradiation for respective male and female nonhuman primates, were 10.24 Gy [9.87, 10.52] (n = 76, male) and 10.28 Gy [9.68, 10.92] (n = 40, female) at two different research sites. The

Corresponding author: Thomas J. MacVittie, MS, PhD., 10 South Pine Street, MSTF 5-02, Baltimore, MD 21201, phone: 410-706-5255; fax: 410-706-5270; tmacvittie@som.umaryland.edu.

The authors declare no conflicts of interest.

respective slopes were steep at 1.73 [0.841, 2.604] and 1.15 [0.65, 1.65] probits per linear dose. The LD50/180 value and slope derived from the dose response relationships for the partial-body irradiation with bone marrow sparing exposure was 9.94 Gy [9.35, 10.29] (n = 87) and 1.21 [0.70, 1.73] probits per linear dose.

A secondary study (1) provided data on limited control cohort of nonhuman primates exposed to whole thorax lung irradiation. The data supported the incidence of clinical, radiographic and histological indices of the dose-dependent lung injury in the nonhuman primates. Tertiary studies (6) provided data derived from collaboration with the noted primary and secondary studies on control cohorts of nonhuman primates exposed to whole thorax lung irradiation and partial-body irradiation with bone marrow sparing exposure. These studies provided a summary of histological evidence of fibrosis, inflammation and reactive/proliferative changes in pneumonocytes characteristic of lung injury and data on biomarkers for radiation-induced lung injury based on matrix-assisted laser desorption ionization - mass spectrometry imaging and gene expression approaches.

Conclusions: The available database in young Rhesus macaques exposed to whole thorax lung irradiation or partial-body irradiation with bone marrow sparing using 6 MV LINAC-derived radiation with medical management showed that the dose response relationships were equivalent relative to the primary endpoint all-cause mortality. Additionally, the latency, incidence, severity and progression of the clinical, radiographic and histological indices of lung injury were comparable. However, the differences between the exposure protocols are remarkable relative to the demonstrated time course between the multiple organ injury of the acute radiation syndrome and that of the delayed effects of acute radiation exposure respectively.

Keywords

health effects; nonhuman primate; radiation effects; mortality

Introduction

Radiation-induced lung injury (RILI) is a recognized delayed effect of acute radiation exposure (DEARE). It is characterized by the development of pneumonitis and pulmonary fibrosis that can lead to respiratory failure, increased morbidity and mortality. It is one of the potentially lethal sub-syndromes that follow acute radiation exposure for victims that survive the more immediate sub-syndromes of the acute radiation syndrome (ARS), including the acute gastrointestinal and hematopoietic sub-syndromes (Prato et al. 1977; Fryer et al. 1978; Van Dyk et al. 1981; Guskova et al. 1990; Baranov et al. 1994; Asano 2005; Uozaki et al. 2005; Dainiak et al. 2011b; Dainiak et al. 2011a; MacVittie et al. 2012; Garofalo et al. 2014a; Cline et al. 2018).

Candidate drugs or biologics, medical countermeasures (MCM), designed to prevent, mitigate or treat organ-specific sequelae of the acute radiation syndrome (ARS) or DEARE cannot ethically be tested in humans and therefore require efficacy testing in well-characterized animal models. These studies are conducted under the Food and Drug Administration (FDA) “Animal Rule” (AR) according to guidance documents set forth by the FDA (Administration 2002). These documents provide expert guidance for the

development and validation of requisite animal models that provide a path to FDA approval licensure of MCM under the FDA AR (Administration 2009; Administration 2015).

Two models, using markedly different irradiation protocols, have recently been developed to assess morbidity and mortality and mitigate RILI in the nonhuman primate (NHP). These models used whole thorax lung irradiation (WTLI) or partial-body irradiation (PBI) with marginal bone marrow (BM) sparing (MacVittie et al. 2012; Garofalo et al. 2014a; Cline et al. 2018; MacVittie et al. 2019a; Thrall et al. 2019).

Development of PBI/BM-sparing and WTLI models utilized both strategic and tactical approaches to assess the natural history of acute radiation effects and efficacy testing of MCM against radiation-induced lung injury. The PBI/BM-sparing model approached the evaluation of delayed effects to the lung as well as kidney, gastrointestinal (GI) and heart within the context of having survived - due to the restoration of the hematopoietic system via the spared BM - the morbidity and mortality of the multiple-organ injury (MOI) within the ARS.

The WTLI model focused on RILI as well as injury to the heart consequent to irradiation of the thorax-only, thus avoiding occurrence of the ARS-MOI characterized by the GI- and hematopoietic (H)-ARS, acute kidney injury (AKI), cachexia and severe immunosuppression (Mackarehtschian et al. 1995; MacVittie et al. 2012; MacVittie et al. 2014; Cui et al. 2016; Cohen et al. 2017; MacVittie et al. 2017; Cohen et al. 2019; Parker et al. 2019a). Although both models can be used to assess RILI and treatment, it is important to consider the potential effect of the MOI of the ARS on the latency, incidence, severity, progression and duration of lung injury using the PBI/BM-sparing vs WTLI model. It is impossible to view RILI using the PBI/BM-sparing exposure protocol in the absence of the fact that those NHP entering the delayed phase post exposure have survived the morbidity and mortality of the ARS MOI and associated delayed effects on other noted organs (Mackarehtschian et al. 1995; MacVittie et al. 2012; MacVittie et al. 2014; Cui et al. 2016; Cohen et al. 2017; MacVittie et al. 2017; Cohen et al. 2019; Parker et al. 2019a; Parker et al. 2019c). In this regard, the NHP exposed using the WTLI protocol did not experience the MOI of ARS during the latent period prior to overt expression of dose- and time-dependent, potentially lethal lung injury. However, WTLI does include the heart and will likely invoke dose- and time-dependent injury that may influence the threshold for RILI (van Luijk et al. 2005; Ghobadi et al. 2012b; de Faria et al. 2015; DeBo et al. 2016).

Methods

Review question. The WTLI vs PBI/BM-sparing exposure protocols in NHP.

What can we learn from the evolution of lethal lung injury characteristic of the DEARE between the two significantly different exposure protocols, PBI/BM-sparing vs WTLI? Our effort herein, was to review and define the development of RILI and MOI in the NHP models using the PBI/BM-sparing protocols with approximately 5% and 2.5% BM-sparing and the WTLI exposure protocol. The database defined the consequences of ARS MOI and its potential influence on the key parameters characteristic of RILI, e.g., the respective latency, incidence, severity and progression of mortality and co-morbidities relative to that

consequent to exposure by WTLI. Our evidence-based advantage within the review of the two predominant exposure protocols is centered on the use of a) young, male or female, rhesus macaques of Chinese origin, to include similar radiation sources; b) veterinary, Institutional Animal Care and Use Committee (IACUC) regulations, c) radiation source and dose rate, d) subject-based medical management, e) euthanasia criteria and f) radiographic, clinical and histological indices of lung injury.

Key questions:

a) Was radiation-induced dose- and time-dependent lung injury equivalent between the models, PBI/BM5 and WTLI? b) Were the clinical, radiographic and histological parameters equivalent relative to latency, incidence, severity and progression between models that had markedly different MOI during the early 60 d time course of ARS that preceded overt lung injury? c) What can we learn from the evolution of lethal lung injury characteristic of the DEARE between the two significantly different exposure protocols, PBI/BM-sparing vs WTLI?

To this end, we assessed the RILI consequent to each exposure protocol, during the 180 d study duration post exposures of 9 to 12 Gy via: a) respective dose response relationships over the 180d study duration, b) analysis of early and delayed effects of acute radiation exposure relative to the respective exposure protocols, c) analysis of the clinical time course of the ARS MOI, d) longitudinal, non-invasive radiographic and clinical evidence of pneumonitis/fibrosis and e) histopathology.

Primary studies, data source.

WTLI model—(Garofalo et al. 2014a; Garofalo et al. 2014b; MacVittie et al. 2017; Thrall et al. 2019).

PBI/BM-sparing model—(MacVittie et al. 2012; MacVittie et al. 2019a).

Animals.

All NHP were young, male or female, Chinese origin rhesus macaques, subspecies Macaca mulatta (4 – 11 kg bw). The primary datasets were derived from contemporary experiments at two sites; the University of Maryland, School of Medicine in Baltimore (UMSOM) and at SNBL, USA, Everett, WA (SNBL) [SNBL now: Altasciences, Overland Park, KS]. A secondary dataset was derived from a recent study at the Wake Forest University, School of Medicine (Cline et al. 2018).

UMSOM studies.—Rhesus macaques, males, (4.0 – 11.0 kg body weight on day of irradiation, n = 76 and n=128) were utilized for the respective WTLI model and PBI/BM5, PBI/BM2.5 model dose-response and selected efficacy studies. All animals underwent quarantine for approximately 90 days and were verified to be in good health, seronegative for simian immunodeficiency virus, simian T cell leukemia virus type 1, malaria and negative for Herpes B virus and Tuberculosis. Animal housing and care have been previously described (MacVittie et al. 2012). *SNBL study*. Rhesus macaques female,(4–6 kg bw, n=40) were used for the WTLI model development. All animals were verified in

good health, were serologically negative for simian immunodeficiency virus, simian T-cell leukemia virus type-1, malaria, herpes B-virus and tuberculosis. Animal housing and care have been previously described (Thrall et al. 2019).

Anesthesia.

Animals were anesthetized with ketamine (Ketaset, 800 5th Street NW, Fort Dodge, IA 50501–7425) [(10 ± 5 milligram (mg) kilogram (kg)$^{--1}$, IM (intramuscularly)] for procedures including initial radiation exposure, CT scans, phlebotomy, physical examinations, and supportive care administration, when necessary. Such procedures were generally performed two to three times per week throughout the in-life phase of the study. For the radiation exposure and CT scans, xylazine (AnaSed, Fort Dodge) [1 ± 0.5 mg kg^{-1}, IM) was administered in combination with ketamine to ensure the animals would remain still for the duration of their exposure. This combination was also administered for other procedures if an animal responded poorly to ketamine as a single agent. Yohimbine (Yobine, 604 West Thomas Avenue, Shenandoah, IA 51601) (0.2 ± 0.1 mg kg^{-1}, IM) was administered to reverse xylazine sedation, if required.

Pre-irradiation procedures and radiation exposure planning.

All NHP underwent a baseline CT scan obtained in the treatment position (supine, in restraint). The pre-exposure CT scan was used to determine and plan the field of irradiation to ensure inclusion of the entirety of both lungs for each animal. Briefly, the CT scan was imported into the radiation planning software platform where the lungs were contoured in 3 dimensions and an appropriate exposure plan and field size. Radiation exposure was prescribed to midplane in the thorax (at the level of the xiphoid) with opposed anteroposterior (AP) and posteroanterior (PA) beams (Garofalo et al. 2014a). Additional pre-exposure activities are described in each study (Cline et al. 2018; Thrall et al. 2019).

Radiation source and quality for exposure protocols: The WTLI vs PBI/BM-sparing exposure protocols.

The primary and secondary studies used 6 MV linear accelerator-derived (LINAC) photons or x-rays to deliver a uniform dose to the same target site, midline tissue (MLT) at the xiphoid process. The PBI/BM-sparing protocols exposed approximately 95 – 97% of the body with approximately 5 – 2.5% BM sparing; the WTLI protocol exposed only the whole thorax region with approximately 35% of active BM exposed (Taketa et al. 1970). The respective dose rates ranged from 0.80 Gy min^{-1} to 2.00 Gy min^{-1} (MacVittie et al. 2012; Garofalo et al. 2014a; MacVittie et al. 2017; Cline et al. 2018; MacVittie et al. 2019b; Thrall et al. 2019). **WTLI exposure protocol.** *UMSOM studies*. NHP (n=76, male macaques) were exposed to a prescribed dose range to the whole thorax at a midline tissue dose of 9.0 Gy (n = 8), 9.5 Gy (n = 10), 10.0 Gy (n = 8), 10.5 Gy (n = 10), 10.74Gy (n = 20), 11.0 Gy (n = 10), 11.5 Gy (n = 6) and 12.0 Gy (n = 4) at a dose rate of 0.80 ± 0.05 Gy min^{-1}. The exposure at 10.74 Gy was used in a contemporary study to assess MCM efficacy. Briefly, the NHP were exposed in an anterior-posterior (AP) / posterior-anterior (PA) technique with approximately 50% dose contribution from both the AP and PA beams. To ensure accuracy of delivery, the NHP were aligned based on the xiphoid mark previously made at time

of the planning CT scan, and a verification AP MV x-ray image was acquired using the LINAC's on-board imager immediately prior to the exposure to verify the planned thoracic field length and width included both lungs in their entirety. Real-time in vivo dosimetry was confirmed with dosimeters (Landauer® nanoDot™ system, Glenwood, IL) placed on each animal at time of exposure. A cylindrical, saline-filled lucite phantom that approximated the mean diameter of the NHP was used to calibrate the LINAC source for midline exposure doses. Real time exposure dose was confirmed with dosimeters (Landauer® nanoDot™ system, 2 Science Rd, Glenwood, IL 60425) placed on each animal at time of irradiation.

SNBL study. NHP (n = 40, female macaques) were exposed to five doses (n=8/dose) (9.0, 10.0, 10.5, 11.0 and 11.5 Gy) of WTLI utilizing 6 MV LINAC-derived photons at a dose rate of approximately 1.0 ± 0.05 Gy min^{-1} (Clinac 21EX, Varian Medical Systems, Palo Alto, CA) as described herein. Irradiation procedures were equivalent to previously published studies (Garofalo et al. 2014a; Kazi et al. 2014; MacVittie et al. 2017). **PBI/BM5 and PBI/BM2.5 exposure protocols**. *UMSOM studies.* Two contemporary studies were designed to determine the dose response relationship (DRR) for mortality vs dose as well as to assess the efficacy of medical countermeasures (MCM), using the partial-body irradiation with the 5% BM sparing (PBI/BM5) exposure protocol. Nonhuman primates (NHP), n = 87, were exposed to doses at 9, 10, 11, 11.5, 12 and 12.5 Gy. The PBI/BM5 protocols determined the slope and lethal dose (LD) values for characteristic MOI of the ARS and DEARE, i.e., acute GI-, H-ARS + prolonged GI damage, AKI and DEARE characterized primarily by lethal lung injury, a cachectic phase through 60 days (d) post exposure and concurrent prolonged GI damage, immune suppression, chronic kidney injury (CKI) and heart injury (MacVittie et al. 2012; MacVittie et al. 2014; de Faria et al. 2015; MacVittie et al. 2015; Cui et al. 2016; Cohen et al. 2017; Cohen et al. 2019; MacVittie et al. 2019a). All control cohorts at respective 10 Gy (n = 15) and 11 Gy (n = 22) doses were combined for complete longitudinal analysis for the PBI/BM5 exposure. A third study was designed to assess the effect of further reduced BM-sparing to ~ 2.5% on the severity of the H-ARS and other acute and delayed multi-organ injury to the GI, lung and kidney (Cohen et al. 2019; Farese et al. 2019; Parker et al. 2019a; Parker et al. 2019c).

Computed tomography (CT).

Serial CT scans provided radiographic evidence of the evolution of lung injury following WTLI and PBI/BM-sparing, both qualitatively and quantitatively. All animals underwent a baseline CT scan to plan their irradiation field, and to assess radiographic evidence of preexisting lung injury or disease prior to study enrollment. Once irradiated, each NHP underwent serial CT scans for surveillance and assessment of RILI, pneumonitis/fibrosis (PF), pleural effusion (PE) or pericardial effusion (PCE) every 30 ± 5 d until the planned end of study (180 d), or at time of "for cause" euthanasia (IACUC criteria) prior to the end of study. Additional scans were acquired when possible, pre- and post-dexamethasone administration. CT scans were acquired and analyzed as described previously using a GE Lightspeed (GE Healthcare Institute, Waukesha, WI) multi-slice CT scanner with a non-contrast enhanced thoracic protocol optimized for lung imaging. Quantification of lung injury was performed in a semi-automated fashion by using the software to assess for differences in characteristic radiodensity [as measured by Hounsfield units (HU)] and

morphology for normal, pneumonitic or fibrotic lung, pleural and pericardial effusion (MacVittie et al. 2012; Garofalo et al. 2014a; MacVittie et al. 2017; MacVittie et al. 2019a). **Assessment of lung injury by clinical parameters.** Radiation induced lung injury is quantified via clinical indices of non-sedated respiratory rate (NSRR), saturation of peripheral oxygen (SpO_2) via pulse oximetry, arterial blood gas and corticosteroid requirements. **Medical management (aka, supportive care).** Supportive care was provided to all study animals as per an IACUC-approved protocol. It was administered to each animal as per clinical signs to initiate and stop treatment. Supportive care included anti-emetics, fluid support, antibiotics, analgesics, antipyretics, anti-diarrheals, anti-ulceratives, corticosteroids, blood transfusions and nutritional support. Treatment of mouth ulcers, diarrhea, anti-emetics, fever and dehydration has been previously described (MacVittie et al. 2012). The WTLI protocol minimized the morbidity consequent to the hematologic and gastrointestinal syndromes by design, therefore supportive care required for these syndromes was minimal. During the conduct of the study presented herein, Invanz® (ertapenem sodium) (Merck & Co. Inc., Whitehouse Station, NJ) was administered in place of Primaxin® when microbial resistance was demonstrated to enrofloxacin, gentamicin, and ceftriaxone. **Hematology**. Peripheral blood was obtained by venipuncture for complete blood counts (CBC) (AcT diff2™, Beckman Coulter, Inc., 11800 SW 147th Avenue, Miami, FL 33196). A white blood cell (WBC) differential, which included verification of all electronically generated WBC < 1,000 cells μL^{-1} was performed by trained personnel using light microscopy and a blood-film stained (Hema- Tek II™, Bayer Corp., Diagnostic Division, 511 Benedict Ave., Tarrytown, NY 10591–5097) with Wright-Giemsa Stain Pack (Fisher Scientific, 2000 Park Lane Dr., Pittsburgh, PA, 15275) on all CBC samples. The absolute neutrophil count (ANC) was calculated (Microsoft Excel 2007) based on the WBC count obtained by CBC and the neutrophil count obtained by manual differential. B**acteriology.** Peripheral blood samples for bacteriology cultures were collected on days when febrile neutropenia (FN), defined as an ANC < 500 cells μL^{-1} coincident with a rectal body temperature ≥ 103.0 °F (39.4 °C), was observed. Blood was cultured in aerobic and anaerobic bottles and analyzed with a BACTEC 9050 Microbial Detection System (Becton Dickinson, 1 Becton Drive, *Franklin Lakes, NJ* 07417–1880). **Corticosteroid administration.** *UMSOM studies.* Dexamethasone (Butler Schein, Dublin, OH) was administered to animals noted to be in respiratory distress [> 80 breaths per minute (bpm)] during daily cage side observations. NHP were treated with a planned taper as follows: 1 mg kg^{-1} IM, twice a day (BID) on the first day of treatment, 0.5 mg kg^{-1} BID for three d, 0.5 mg kg^{-1} once a d (QD) for three d, and 0.5 mg kg^{-1} every other d (QOD) for three doses. The dexamethasone treatment paradigm is described previously (Garofalo et al. 2014a; MacVittie et al. 2017). *SNBL study*. Clinical signs dictated the initiation and cessation of medical management administered to each NHP as per the published studies performed at University of Maryland. The dexamethasone treatment paradigm followed that used within the UMSOM studies (Garofalo et al. 2014a; MacVittie et al. 2017; Thrall et al. 2019).

Histopathologic evidence of pneumonitis and fibrosis.

Necropsy tissues were analyzed from the lungs of all euthanized animals. Three or more sections were procured from each lung according to a prescribed protocol. These formalin-

fixed sections were stained with hematoxylin and eosin (H&E), Masson-Trichrome (M-T), Coll-1 via IHC, alpha-SMA, TGF-beta, connective tissue growth factor (CTGF) and others (Parker et al. 2019c; Thrall et al. 2019). Pneumonitis, per se was based on histologic evidence of leucocyte/macrophage infiltration with associated tissue alterations. Fibrosis was based primarily on demonstration of fibrous connective tissue with M-T staining, with supportive indications from immunohistochemistry (IHC) staining for collagen-1 and alpha smooth muscle actin (SMA). **Euthanasia.** *UMSOM studies.* Animals were euthanized based on IACUC-defined clinical criteria. Specifically, the criteria included persistent loss of body weight, hyperthermia or hypothermia that was unresponsive to therapy, evidence of self-mutilation, evidence of unrelieved pain or stress, seizure activity, abnormal activity and respiratory distress. Animals are euthanized by the administration of a Drug Enforcement Agency Class III euthanasia solution (Euthasol®, Virbac AH Inc., Ft. Worth, TX) (0.27 mL kg^{-1}, IV). *SNBL study.* The criteria for euthanasia were explicitly defined to avoid bias. Euthanasia criteria included any one of the following observations: indication of unrelieved pain or distress following administration of two consecutive increased doses of buprenorphine (0.02 mg kg^{-1} IM BID), inactivity (e.g., recumbent in the cage for at least 15 min, or non-responsive to touch), uncontrolled hemorrhage from any orifice, or severe dehydration as determined by veterinarian examination. Non-absolute euthanasia criteria included any combination of two or more of the following observations: tachypnea (e.g., ≥ 60 bpm and unresponsive to treatment, bw loss ≥ 25% of pre-irradiation baseline for two consecutive d, observations of severe injury or condition (e.g., minor bone fracture, progressive tissue necrosis, non-healing wound), hyperthermia (rectal temperature ≥ 41°C), hypothermia (rectal temperature ≤ 35°C), or complete anorexia for 48 hr. Moribund animals and surviving animals at post irradiation d 180 were sedated and then euthanized by intravenous (IV) injection of a pentobarbital overdose. **Survival.** Mortality due to RILI/MOI was defined at 180 d post exposure. Acute gastrointestinal (GI)-ARS survival was defined at 15 d post-irradiation, and acute hematopoietic (H)-ARS survival was defined at 60 d post-irradiation. **Statistics.** Probit fits were made to mortality data, and confidence intervals were calculated for LD and slope values according to the methods of Finney using the R statistical software (version 2.13.1.) (Finney 1947). A comparison of slopes and LD50s was made using Wald statistics. Means values and associated standard errors for continuous and count data were calculated and plotted using Microsoft Excel 2010 (MacVittie et al. 2012; Garofalo et al. 2014a; Garofalo et al. 2014b; MacVittie et al. 2017; MacVittie et al. 2019a; Thrall et al. 2019).

Secondary data source.

Cline (2018).—The study used a NHP model of WTLI to evaluate the efficacy and safety of a potential MCM (Cline et al. 2018). **Animals:** Five of a total 16 juvenile, Chinese-origin, male, rhesus macaques, (average wt 3.9 kg) were exposed to 10 Gy WTLI as the control cohort. **Radiation exposure:** The NHP exposure used parallel-opposed anterior and posterior beams of 6 Mev x-rays from a clinical linear accelerator at a nominal dose rate of 2.00 Gy min^{-1} delivered at the midline (xiphoid process). Further exposure parameters are provided in the reference. **Clinical Assessments:** Animals were observed daily throughout the study. Respiratory rate (RR) and effort were evaluated daily. Animals were assessed for CBC and serum chemistries to include blood urea nitrogen (BUN)

and creatinine. Oxygenation by pulse oximetry was documented weekly. **Subject-based clinical indices of pneumonitis and administration of corticosteroids:** NHP with RR > 80 bpm were treated with corticosteroids (prednisone, 1 mg kg^{-1} d, tapered). Normal RR was 50 bpm. **Medical management, euthanasia**: Subject-based supportive fluid therapy, corticosteroids, analgesics, antibiotics, and other symptomatic care were given based on clinical signs and clinical pathology findings. **Euthanasia criteria**: Relevant thresholds for treatment or humane euthanasia were followed (NHP with RR > 100 bpm were euthanized) as per IACUC criteria. **Radiographic imaging:** CT was utilized prior to irradiation and at two and four mo after irradiation. The lungs were fully inflated during the scan to avoid motion artifacts. Three-dimensional reconstruction and volumetric calculations were used to determine the proportion of the lung occupied by air, normal lung tissue, and abnormally dense tissue. **Pathology: Clinical Observations**: Mean RR increased gradually post exposure, reaching statistical significance by 4 mo ($P < 0.009$). The mean number of days to corticosteroid treatment was 51 d (range, 26 – 77 d) for the 10 Gy cohort. The SpO_2 values did not change over the course of the study which suggested compensation by an increased RR. One of five NHP was euthanized at 4 mo due to respiratory insufficiency [non-sedated (NS) RR > 100 bpm]. Remaining NHP were euthanized as scheduled at 4.5 mo post exposure. **CT Imaging:** Imaging abnormalities, defined as abnormal radio-opacities exceeding 1% of the lung volume, were seen two mo after irradiation in two of five irradiated-animals. Abnormalities were seen in all irradiated animals at four mo after irradiation. These consisted of multifocal, irregular, randomly distributed areas of increased radio-opacity in all lung lobes, which progressed in severity during the study. **Histology**: Histologically, affected regions of the lung in irradiated animals contained four major changes: (1) interstitial and intra-alveolar infiltration of the lung parenchyma by macrophages and other inflammatory cells, (2) accumulation of proteinaceous fluid in alveolar spaces, (3) hyperplasia and hypertrophy of alveolar lining cells, leading to the replacement of the normal thin oxygen exchange layer of type I pneumocytes with a thicker layer of cuboidal Type II cells, and (4) fibrosis of the pulmonary interstitium. A clinical and pathologic pattern of disease progression was similar to that observed in human disease. **Gross necropsy:** Abnormalities consisted of increased lung weights, abnormally firm lung consistency on palpation, and multifocal to diffuse, gray to tan discoloration of the pulmonary parenchyma that involved up to approximately 90% of the lung parenchyma. Lung weights were 77% higher than non-irradiated controls ($P < 0.0001$). CT density correlated with elevated respiratory rate ($r = 0.629$, $P < 0.009$) at the 4 mo assessment. Cline and colleagues stated that their findings in the 10 Gy control cohort were consistent with that shown by the Garofalo team relative to progressive pneumonitis and pulmonary fibrosis by 4 mo post 10 Gy exposure (Garofalo et al. 2014a).

Results and Discussion

The Mortality dose response relationship (DRR): PBI/BM5 relative to WTLI.

The DRR for mortality was comparable in the two predominant NHP models using either PBI/BM5 or WTLI exposure protocols (Fig. 1, Table 1). The respective LD50/180 values are 9.94 Gy [9.93, 10.29] (n = 87) and 10.24 Gy [9.87, 10.52] (n = 76) for the studies conducted in male NHP at UMSOM. The respective slopes were approximate at 1.21 and

1.15. The DRR for the study conducted at SNBL in female NHP, resulted in an LD50/180 of 10.28 Gy [9.68, 10.92] (n = 40) with a slope of 1.72. The NHP, male or female, exposed to WTLI protocols expressed RILI with comparable dose- and time-dependent, morbidity and mortality across the lethal dose range over the 180 d study duration. The respective DRRs for the WTLI exposures conducted at UMSOM and SNBL are not significantly different from each other ($P = 0.25$, Chi square). Similarly, the comparison of the slopes and LD50/180 values from the PBI/BM5 and WTLI exposures performed at UMSOM showed no statistical difference in slope (P = 0.85) or intercept (P = 0.15). There is no significant difference between the LD50/180 values or the slopes of the DRR's between the PBI/BM5 or WTLI exposure protocols (P = 0.86). There is an approximate zero shift between the probit lines.

The respective LD values are presented for LD30, LD50, LD70, slope, and total number of animals used in determining the DRR. The values for the DRR are derived from linear normal probit fits. LD values are given with 95% confidence intervals in brackets (Fig. 1).

Note: *There is no significant difference between the LD50/180 values or the slopes of the DRR's between the PBI/BM5 or WTLI exposure protocols (P = 0.86).* There is an approximate zero shift between the probit lines and essentially the two probit data sets could be combined. This data presents an alternative view of the evolution of delayed MOI within the two exposure protocols. An initial approach centered on the assumption that the DRR for the lung-DEARE induced by the PBI/BM5 exposure protocol would be significantly affected by the early morbidity and mortality due to the MOI of the ARS. The WTLI protocol was designed to focus on the lung (plus heart) and spare all the early and prolonged sequelae associated with the ARS and thus present a model focused on acute irradiation of only the lung and heart. The PBI/BM2.5 exposure protocol used only a single dose of 10 Gy. The sparing of less BM, ~ 2.5% vs ~ 5%, shifted the all-cause mortality at 180 d due to the respective increased H-ARS plus GI-ARS mortality within the initial 60 d (58% vs 27%) post exposure (Fig. 1, Table 2).

Mortality, Kaplan-Meier Analysis: The PBI/BM-sparing protocols relative to WTLI exposure protocol, interactive biology.

Comparison of survival outcome in the three established models, PBI/BM5, PBI/BM2.5 or WTLI provided insight into the timeline and severity of the GI- and H-ARS sub-syndromes and associated co-morbidities due to radiation-induced MOI (AKI, cachexia, and prolonged immune suppression) that may modulate the time course and severity of the delayed lung and associated MOI (MacVittie et al. 2012; MacVittie et al. 2015; Cui et al. 2016; Cohen et al. 2017; MacVittie et al. 2017; Cohen et al. 2019; Parker et al. 2019a). The percentage of BM-spared, modulated the dose-dependent "all-cause" survival probability relative to "organ-specific" morality (Fig. 2, Table 2). Note that the delayed mortality due to RILI was associated with cardiac injury, CKI and prolonged GI, CKI damage and immune suppression through the 180 d study duration (MacVittie et al. 2012; MacVittie et al. 2014; de Faria et al. 2015; Cui et al. 2016; Cohen et al. 2017; Cohen et al. 2019; Farese et al. 2019; Parker et al. 2019a; Parker et al. 2019c). The recent description of AKI and CKI in the PBI/BM-sparing protocols has placed additional emphasis on defining the interaction between

acute radiation-induced kidney injury and the lung and heart. Any number of cellular and mediator-based mechanisms have been suggested to include recent studies focused on a cyto-protective and anti-oxidative mediator called alpha-Klotho produced by the kidney. These combined injuries may modulate the time course and severity of the delayed lung injury (van Luijk et al. 2005; Faubel 2008; Ghobadi et al. 2012b; de Faria et al. 2015; Faubel and Edelstein 2016; Hsia et al. 2017).

PBI/BM-sparing, time course of mortality.

The Kaplan-Meier plots demonstrated the relative effects of dose, and exposure protocol over the critical time segments that defined survival probability for cohorts of the PBI/BM-sparing protocols over the 180 d study duration (Fig. 2). There is a differential effect of time, radiation dose and an approximate, marginal 2.5% relative to an approximate 5% BM-sparing on the survival probability over the 180 d study duration (Fig. 2). The PBI/BM5 protocol reduced survival after 10 Gy or 11 Gy to 47% and 14% respectively, after the 180 d duration. Sparing only an approximate 2.5% at an exposure of 10 Gy reduced survival to 8% relative to the 47% noted for the 10 Gy using the BM5 protocol (Table 2). The sparing of a marginal 2.5% of active BM, likely approached the threshold for the survival-enhancing effect of spared BM. Note: the exposure protocol for PBI/BM-sparing resulted in an approximate 0.50 Gy dose to the “spared tibial BM”. The D_{37} for the hematopoietic “stem cell” has been estimated at 0.60 Gy (van Bekkum 1991). The 12 Gy exposure, an estimated LD50/15 for the PBI/BM5 and PBI/BM2.5 protocols were equivalent in the early acute GI-ARS lethality. The survivors of the acute GI-ARS within the PBI/BM5 protocol experienced longer survival time, through the H-ARS + GI injury to eventual 100% lethality within 100 d post exposure (Fig. 2).

The early phase of morbidity and mortality noted within the time course of the ARS, 1–60 d post exposure, reflected the influence of the concomitant GI- and H-ARS and associated morbidities on the longitudinal increase of all-cause mortality in the PBI/BM5 and PBI/BM2.5 models.

WTLI, time course of mortality.

The time course of mortality within the WTLI model was characterized by the early latent, clinically silent period due to the sparing of high-dose exposure to the BM, GI and kidney and the absence of the overt ARS and associated morbidities (Fig. 3, Table 2). The latent period for the WTLI cohorts coincided with the evolution of the lethal ARS and associated morbidities noted in the PBI/BM-sparing models. Thereafter, the continued loss of survival probability was associated with overt lung injury in both PBI/BM-sparing and WTLI models as shown in both the UMSOM and SNBL studies (MacVittie et al. 2012; Garofalo et al. 2014a; MacVittie et al. 2019a; Thrall et al. 2019). Cline and colleagues reported one death of five (20%) NHP due respiratory insufficiency (NSRR > 100 bpm) at 120 d post 10 Gy WTLI. The remaining, four NHP, were euthanized at the scheduled at 4.5 mo (~ 135 d) study duration; which was ~ 45 d less than the duration of the UMSOM- and SNBL-directed studies (Cline et al. 2018). The probit analysis from the respective SNBL and UMSOM studies estimated ~ 30 – 40% mortality at 10 Gy WTLI within the longer, 180 d study duration used at UMSOM and SNBL (Fig. 1).

Exposure to the dose range from 10.5 Gy to 11.0 Gy resulted in 60% to 80% mortality for NHP exposed using the WTLI model. Exposure to 10 Gy or 11 Gy using the PBI/BM5 model resulted in 53% and 86% all-cause mortality relative to 92% all-cause mortality using 10 Gy delivered via the PBI/BM2.5 protocol over the 180d study duration, respectively (Table 2). Mortality, using either the PBI/BM5 or WTLI model was approximate relative to the respective DRRs and longitudinal analysis for lung injury as evidenced in the Kaplan-Meier plots and euthanasia relative to lung injury and respiratory insufficiency. The mortality at 180 d associated with the PBI/BM2.5 model (92%) was greater than that noted in the PBI/BM5 model (53%) due to the greater, early mortality noted within 60 d post exposure for the PBI/BM2.5, i.e., 58% vs 27% for the PBI/BM5 protocol (Table 2).

PBI/BM-sparing models, co-morbidities. The ARS MOI time segment: A presentation of clinical signs combined for NHP consequent to 10 Gy and 11 Gy PBI/BM5 exposure.

Exposure to 10 Gy or 11 Gy with the PBI/BM-sparing protocols resulted in a qualitatively equivalent time course of MOI within the ARS (Fig. 4). The PBI/BM-sparing exposure protocols resulted in a definitive pattern of the incidence, severity and progression of mortality and clinical signs of morbidity, i.e., dehydration, mucositis, loss of body weight (anorexic plus cachectic), diarrhea, increased BUN, creatinine and late occurring edema, increased plasma-based cytokines/chemokines and mediators and mucositis. These clinical signs are predominant throughout the concomitant evolution of the acute GI- and H-ARS, severe immunosuppression and AKI through the first 60 d post exposure (Fig. 4). The acute MOI is coincident with the latent period for MOI of the DEARE. Note that clinical, trigger-based, medical management was provided throughout the 60 d post exposure. The graphic illustrates the marked disruption in multiple biological systems to include mortality that are predominant throughout the latent period for MOI characteristic of the DEARE, e.g., lung, kidney, prolonged GI, immunosuppression and heart injury (MacVittie et al. 2012; MacVittie et al. 2014; de Faria et al. 2015; Cui et al. 2016; Cohen et al. 2017; Cohen et al. 2019; Farese et al. 2019; Parker et al. 2019a).

These overt signs of acute radiation effects defined the relatively silent or latent period prior to the overt evolution of MOI characteristic of the DEARE. A critical gap in knowledge is whether the overt signs during the latent period effected the latency, incidence, severity and time course of the DEARE to include the ability of biomarkers to predict clinical outcome.

The ARS timeline for MOI within the PBI/BM5 and PBI/BM2.5 protocols was associated with concomitant co-morbidities that contributed to IACUC-approved euthanasia criteria (Table 3). The euthanasia criteria noted for the associated ARS MOI and co-morbidity in the PBI/BM-sparing models accounted for approximately 20% additional mortality over the 60 d time segment post exposure. Whereas, the morbidity and mortality due to RILI remained unchanged for WTLI exposure models during the extended latent period of approximately 40 – 60 d post exposure. Thereafter, the dose-dependent incidence of mortality due to lung injury increased and progressed through the 180 d study duration for NHP exposed via either PBI/BM-sparing or WTLI protocols.

WTLI with significant BM-sparing and marginal co-morbidities.

Hematologic parameters.—Given that only 30 – 35% of the BM in the NHP is irradiated in the thoracic field, we hypothesized that the NHP in the WTLI studies would largely avoid any clinically significant hematopoietic injury (Taketa et al. 1970). The radiation-induced cytopenia and febrile neutropenia are hallmarks of the acute H-ARS. Incidence and duration of neutropenia and thrombocytopenia have been shown to be important secondary endpoints in total-body irradiation models of the H-ARS and GI-ARS. NHP exposed to WTLI protocol in the 9.0 – 12.0 Gy range did not develop neutropenia or thrombocytopenia (data not shown).

Incidence of diarrhea.—Given that the WTLI exposure geometry largely excluded the abdomen, the incidence of diarrhea was relatively low. Stool consistency was scored twice daily based on an established grading scale. Furthermore, there was no bloody diarrhea seen in any cohort which was attributable to the marginal GI effect and replete component of functional platelets (Fig. 5).

These results underscored the marked difference in acute radiation-induced, early organ-based sequelae and co-morbidities between the two exposure protocols, PBI/BM-sparing and WTLI. The Medhora and Fish team demonstrated an approximate relationship in the WAG/RijCmcr rat model, given the differences in species-dependent radiation sensitivity, biology and modified medical management (Jacobs et al. 2019; Fish et al. 2020).

The ARS and DEARE MOI: Early and delayed clinical signs of co-morbidity and mortality - a combined database - 1–60d and 60–180d post 10 Gy PBI/BM2.5 or 10 Gy and 11 Gy PBI/BM5 exposure protocols.

The animal model research platform using the PBI/BM-sparing protocols shifted the mortality DRR for both the acute GI- and H-ARS in the mouse, rat and NHP and also the DRR for delayed MOI chracterized primarily by morbidity and mortality of lung, kidney and heart injury (Booth, Tudor, Tonge, 2012; Fish, MacVittie, 2020; MacVittie, Bennett, 2012;(Farese et al. 2012; Boittin et al. 2015; de Faria et al. 2015; Medhora et al. 2015; Fish et al. 2016; Cohen et al. 2017; Cohen et al. 2019; Jacobs et al. 2019; MacVittie et al. 2019b; Parker et al. 2019a; Parker et al. 2019b; Parker et al. 2019c). The respective DRRs shifted the LD50/30 for the WAG rat from ~ 7.5 to 12.7 Gy and the LD50/60 for NHP from 7.4 to 10.9 Gy. The models established with PBI/BM-sparing permitted the analysis of concomitant and concurrent dose- and time-dependent development of multiple organ-specific sequelae and mortality within the ARS and DEARE (Fig. 6). Mortality due to the H-ARS was shifted to the threshold range for GI-ARS-induced mortality and DEARE.

Biomarker consideration: *Furthermore, the "early phase" is a critical period for identification of key biomarkers that can predict delayed clinical outcome relative to MOI.* To this end, selective time segments will be analyzed relative to all clinical, radiographic, plasma-based cytokines/chemokines and mediators, histological tissue and cellular-based parameters as well as multi-disciplinary biomarker analysis in a focused effort to develop a biomarker paradigm that will predict clinical outcome. *It is imperative to note that these overt signs of acute radiation effects define the relatively silent or latent period prior to the*

overt evolution of MOI characteristic of the DEARE. A critical gap in knowledge is whether the overt signs during this latent period effect the incidence and time course of the DEARE to include the ability of biomarkers to predict clinical outcome.due to delayed MOI (Figs. 4, 5, 6).

The relatively high-dose exposure required for threshold doses to induce injury to lung, kidney and heart characteristic of the DEARE resulted in respective latent periods characterized by the presence or absence of a significant, acute, systems biology response. The comparative analysis of the evolution of RILI in these models will provide a database to assess the influence of potentially lethal, acute MOI and co-morbidities within the time course of the ARS on the latency, incidence, severity and progression of RILI and associated MOI to the kidney and heart. Additionally, the PBI/BM-sparing models included the concomitant evolution of CKI with that of injury to the lung and heart. Thus, the PBI/BM-sparing models established a radiation-induced, interactive environment, between three major organ systems, the lung, kidney and heart (van Luijk et al. 2005; Faubel 2008; Ghobadi et al. 2012a; de Faria et al. 2015; Faubel and Edelstein 2016; Hsia et al. 2017) (Fig. 6).

It is of interest that a summary analysis to this point indicated there is no significant difference in the DRR for the PBI/BM5 vs WTLI models (MacVittie et al. 2012; Garofalo et al. 2014a; Garofalo et al. 2014b; MacVittie et al. 2017; MacVittie et al. 2019a; Thrall et al. 2019). The LD50/180 values and slopes are essentially equivalent (P = 0.86), there is an approximate zero shift between the probit lines **(**Fig. 1).

Mean survival time (MST) of decedents due to RILI, greater than 60 d post exposure. WTLI protocols.

The MST of decedents decreased in an inverse relationship with the increasing dose of WTLI in both the UMSOM and SNBL studies. The MST for dose-dependent cohorts in the UMSOM study were 9.5 Gy, 176.5 d; 10.0 Gy, 127.8 d; 10.5 Gy, 114.0 d; 10.74 Gy, 106.5 d; 11.0 Gy, 86.2 d; 11.5 Gy, 107.0 d; 12 Gy, 89.8 d, respectively (Garofalo et al. 2014a; Garofalo et al. 2014b; MacVittie et al. 2017). The longer MST observed in the 11.5 Gy cohort may be a result of an earlier mean first day of dexamethasone administration (76 d) as compared to the 11.0 Gy cohort (90 d) (Table 4). The MST for comparable dose-dependent cohorts in the SNBL study were 10.0 Gy, 151.5 d; 10.5 Gy, 99.6 d, and 11.0 Gy, 102.1 d and 11.5 Gy, 81.5 d, respectively (Thrall et al. 2019) (Table 5). The study by Cline and colleagues had a single death at 10 Gy at 120 d post exposure (Cline et al. 2018). ***PBI/BM-sparing protocols***. The MST of decedents decreased with the increasing dose in the PBI/BM-sparing exposure protocols. The respective dose and MST for the PBI/BM5 cohorts were, 10.0 Gy, 126.8 d and 11.0 Gy, 125.1 d. The MST for PBI/BM2.5 cohort exposed to 10 Gy was 115.4 d. (MacVittie et al. 2012; MacVittie et al. 2019a). **Summary:** The MST relative to dose delivered to the prescribed target were comparable in NHP exposed to either protocol, the PBI/BM-sparing or WTLI (Table 5). All NHP were administered trigger- and subject-based medical management to include dexamethasone that influenced MST. The database was also affected by loss of NHP and therefore reduced survivors along the time course post exposure.

Dose distribution to the lung, kidney and heart: The prescribed dose relative to the organ-specific and descriptive dose for PBI/BM-sparing and WTLI of the NHP.

The average dose to an organ volume varied relative to the prescribed, uniform, bilateral dose delivered at the target site in the PBI/BM-sparing and WTLI exposure protocols (Prado et al. 2015; Prado et al. 2017). The DRR for MOI in the ARS and DEARE have been equated to a prescribed and descriptive dose at a single point which may or may not be reflective of the actual dose received throughout the organ of interest, in this case, the lung. True DRRs can be calculated using three-dimensional dose calculations combined with tissue heterogeneity corrections. This approach permitted precise measurements of specific volume or organ tissue and the dose received within that volume.

Prado and colleagues evaluated the dose to lung, kidney and heart in the PBI/BM2.5 and WTLI exposure protocols described herein. The prescribed dose used in the PBI/BM2.5 protocol was 10.0 Gy, delivered to midline tissue at the xiphoid process. This was the exact exposure design used for the PBI/BM5 protocol. However, using the CT-based heterogeneity analysis, the mean organ dose to lung was 10.62 Gy with a (min, max dose) of 9.67 Gy and 11.20 Gy. The respective mean doses (and min, max doses) to the kidney and heart were 10.71 Gy (10.06, 11.11) and 10.51 Gy (10.07, 10.92). The variation in organ dose after uniform, bilateral, WTLI exposure as described herein was assessed in a cohort that received a prescribed dose of 10.74 Gy. The mean lung dose averaged across all NHP was 11.05 Gy with a min/max of 10.00, 11.67 Gy (Prado et al. 2015; Prado et al. 2017). The respective mean (n = 12 NHP) organ volumes were 210 cc, 35 cc and 56.2 cc for lung, kidney and heart

Summary: This approach showed that the organ-specific pathology could be connected to the dose delivered to the specific organ volume and to the prescribed dose at standard target midline tissue, i.e., the stated, descriptive, “whole body dose” or “partial-body dose”. The relationship between the prescribed dose and the dose delivered to the organ-specific volume may be modified by variables not considered herein, e.g., radiation quality and characteristics, uniformity of dose delivery, animal size and age.

WTLI and PBI/BM-sparing control cohorts: Clinical evidence of RILI. Radiation pneumopathy: incidence and latency.

The latency to development of clinical pneumopathy [pneumonitis (inflammation) and tachypnea] was calculated in the PBI/BM-sparing and WTLI studies based on the elapsed time from initial radiation exposure to development of tachypnea and respiratory distress (defined as a NSRR of > 80 bpm in room air). Therefore, this analysis was restricted to NHP for whom complete, serial NSRR data were available post WTLI and among those NHP who survived the ARS MOI noted within the latent period for lung injury in the PBI/BM-sparing models in both the UMSOM and SNBL studies. Additional support for assessing time course of compromised respiratory function was evidenced by diminished SpO_2 and arterial blood gas.

SpO_2, pulse oximetry, arterial blood gas analysis.

The change in SpO_2 was an indicator of compensated respiratory function. Lethality in the WTLI model was consequent to pulmonary injury and respiratory failure. Hypoxia, as

evidenced by low SpO_2, was the most common single IACUC euthanasia criteria met for decedent NHP in this and other contemporary UMSOM comparative studies (Fig. 7 a, b) (Garofalo et al. 2014a; Garofalo et al. 2014b; MacVittie et al. 2017). The SNBL study used arterial blood gas rather than SpO_2 for all NHP. The arterial partial pressure of oxygen (PO_2) trended downward post-irradiation compared to baseline values and indicated impaired gas exchange between alveolar air and pulmonary capillary blood (Thrall et al. 2019). This decrease was more pronounced in non-survivors euthanized during the study than survivors through the 180 d duration. Cline and colleagues reported in the NHP exposed to 10 Gy, that the SpO_2 values did not change over the course of the study which suggested compensation by an increased respiratory rate (Cline et al. 2018).

NSRR, tachypnea: UMSOM studies, WTLI and PBI/BM-sparing cohorts.

The mean baseline, pre-irradiation values for cohorts exposed to WTLI or PBI/BM-sparing, ranged from 33–37 bpm. The mean NSRR for all irradiated NHP remained within baseline values through approximately 30 – 40 d post exposure (Figs. 8a, b; 9a, b). This suggested RILI was clinically silent for approximately 1 mo following exposure in the dose range of 10 Gy to 11 Gy regardless of the exposure protocol, WTLI or PBI/BM-sparing. The mean NSRR increased steadily to 60 bpm thereafter in the majority of NHP; an initial indication of breathing difficulty. The first day to reach 60 bpm was approximately 104 d and 94 d in the PBI/BM5 10 Gy and 11 Gy cohorts and 98d in the 10 Gy PBI/BM2.5 cohort. Those NHP in which NSRR continued to rise, reached 80 bpm (clinical sign of tachypnea), the primary trigger for initiation of dexamethasone administration, at 128 d and 98 d, respectively for the 10 Gy and 11 Gy cohorts exposed with PBI/BM5 and 98 d in the 10 Gy PBI/BM2.5 cohort (Figs. 8a, b; 9a, b; Table 4). The WTLI cohorts exposed to 10 Gy, 10.74 or 11 Gy reached the 80 bpm, trigger-to treat with dexamethasone, within 117 d, 78 d and 90 d, respectively (Table 4).

Dexamethasone administration.

The subject-based administration of dexamethasone had a variable influence on the longitudinal expression of NSRR irrespective of the dose and exposure protocol, WTLI or PBI/BM-sparing. Dexamethasone was generally effective in temporarily palliating the symptoms of radiation-induced pneumonitis as reflected in secondary end points such as NSRR, arterial blood gas (PO_2) and radiographic CT evidence of lung injury (MacVittie et al. 2012; Garofalo et al. 2014a; MacVittie et al. 2017; MacVittie et al. 2019a; Thrall et al. 2019). Graphically, this mitigation is evident when one overlays the mean latency to onset of clinical pneumonitis and mortality, e.g., initial dexamethasone treatment with the mean NSRR and mortality for both WTLI and PBI/BM-sparing protocols (Figs. 8a, b, 9a, b).

SNBL study, WTLI cohorts.

The dexamethasone support regimen administered at SNBL was equivalent to the UMSOM study; subject-based and initiated when the NHP developed clinical evidence of lung injury e.g., an NSRR > 80 bpm. The first day to dexamethasone administration for the comparable 10 and 11 Gy exposures were 114 d and 117 d and 80 d and 90 d for the SNBL and UMSOM studies, respectively (Figs. 8a, b; 9a, b, Table 4). The data indicated that, for

similar radiation doses (10. 10.5, 10.74 and 11 Gy), breathing rates and dexamethasone administration was analogous for both studies using the WTLI exposure protocol.

Cline and colleagues indicated that prednisone was less effective in reducing respiratory rate in their study. A similar trigger for NSRR was used to initiate use of the corticosteroid. Furthermore, the median first day to use of corticosteroids was 51 d versus mean first days of 117 d and 114 d in respective UMSOM and SNBL studies (Cline et al. 2018). The age of the NHP may account for this variance. Cline et al., used juvenile NHP with a resting NSRR of ~ 50 bpm relative to that of 33 – 37 bpm for the NHP used in the UMSOM and SNBL studies. It was suggested that radiation sensitivity may be age-dependent, generally adolescent rats develop pneumonitis more rapidly than adult animals (Mahmood et al. 2013).

Summary.

The latency to development of clinical pneumopathy [pneumonitis (inflammation) and tachypnea] was calculated based on the elapsed time from radiation exposure to development of tachypnea and respiratory distress (defined as NSRR of > 80 bpm, in room air). The NSRR and tachypnea recorded from all eligible NHP remained within baseline values through approximately 50 d post exposure. Therefore, RILI was clinically silent for approximately 2 mo following exposure to threshold doses within either the PBI/BM-sparing or WTLI exposure protocols. Mean NSRR values increased steadily thereafter to reach a positive signal for early breathing difficulty when the majority of NHP reached an NSRR of 60 bpm which ranged from 50 – 100 days. The first clinical sign of tachypnea (80 bpm), the primary trigger for initiation of dexamethasone administration was dose-dependent and similar within respective cohorts regardless of exposure using the PBI/BM-sparing or WTLI protocols.

The time course of clinical indices of pneumonitis, NSRR, dexamethasone administration and mortality: PBI/BM-sparing and WTLI exposure protocols.

The trend towards lessening mean NSRR beyond d 90 post exposure using either exposure protocol was explained by the effective treatment with corticosteroids and the progressive lung injury and mortality of the most severely affected NHP. The NSRRs for irradiated cohorts are shown relative to the respective Kaplan-Meier survival plots (Fig. 8 a, b). As noted earlier, the mean values for NSRR increased steadily within the serial 70–120 d time segments when mortality due to dose-dependent lung injury was increasing. All animals diagnosed as having developed pneumopathy (tachypnea) based on clinical signs had correlative radiographic and histopathologic evidence of lung injury over the equivalent time course of mortality.

Summary comments:

The subject-based administration of dexamethasone based on the trigger-to-treat, mitigated pneumonitis, as shown by the decreased NSRR (also shown in radiographic analysis). The results suggested that decedent MST may be increased with dexamethasone administration but not overall survival at 180 d. There are no comparable published studies without the use of dexamethasone support. The effect of dexamethasone on long-term survival is not known. In this context, use of dexamethasone likely mitigated other organ- and

cellular-based inflammation and induction of fibrosis. This underscored the strategic view of radiation-induced MOI and assessing the use of medical management, e.g., corticosteroids during the concomitant evolution of MOI and use of MCM. The time course of the rise in NSRR and initiation of dexamethasone treatment correlated with the decrease in survival probability associated with the time course of RILI and MOI.

Knowledge gap: Will the use of subject-, trigger-based medical management have significant effects during the latency, incidence, severity and progression of delayed MOI? The database herein suggested that morbidity and mortality due to acute RILI and associated MOI, may be due to organ-specific, systems biology, focused in initiating RILI that may not be influenced by other concomitant multi-organ sequelae that precede the overt incidence of lung injury. The latent period for RILI and DEARE-MOI within the NHP exposed to PBI/BM-sparing or WTLI protocols may be defined by effects on biological systems that are independent of the early ARS-MOI and morbidity.

WTLI and PBI/BM-sparing control cohorts: Radiographic evidence of radiation-induced lung injury. The incidence, time course, severity and progression of lung injury, pneumonitis, fibrosis and pleural effusion.

Radiographic evidence of lung injury was reported quantitatively as ratios of PF and PE to total lung volume (TLV). The PF:TLV and PE:TLV represented the percentage of lung that appeared injured, PF or acquired PE relative to respective TLV at the time the CT scans were taken over the respective time course after WTLI or PBI/BM-sparing exposures. It was important to index the injury against the TLV due to the variability of TLV noted at dominant phase of respirations during the scan (Garofalo et al. 2014a; Garofalo et al. 2014b; MacVittie et al. 2017; MacVittie et al. 2019a).

WTLI exposure protocol: Evolution of radiographic changes: PF:TLV, PE:TLV. Radiographic evidence of RILI as PF and PE evolved with time over the 180 d study duration after potentially lethal WTLI in all NHP. Serial images were obtained at three different locations in the lung, apex, mid-lung and base from surviving NHP euthanized at the end of the 180 d study. These images provided evidence of the marked regional heterogeneity in tissue damage during the progression of RILI in lungs of representative NHP (Garofalo et al. 2014a). Dexamethasone treatment is known to influence lung injury and its radiographic appearance (Phillips et al. 1975; Gross 1980; Gross et al. 1988; Berkely 2010; Garofalo et al. 2014a). PF:TLV: Overall incidence of radiographic injury. The longitudinal radiographic data revealed the resolute presence of RILI in all irradiated control cohorts. Radiographic evidence of PF was evident at the initial CT scans at 30 d post-irradiation and ranged from 20% to 55% across all cohorts. The PF:TLV mean values for lung injury for all NHP (survivors and non-survivors) increased to reach a plateau from 90 to 180 d post-irradiation. The longitudinal analysis demonstrated the intractable persistence of lung injury consequent to a lethal (50 – 70%) dose WTLI (Fig. 10a).

Cline and colleagues assessed radiographic indices at baseline, then 2 and 4 mo post exposure. Abnormal radio-opacities were seen in 2 of 5 NHP at two mo and in all 5 NHP at 4 mo post WTLI at 10 Gy. The opacities increased in severity with post exposure and

consisted of multifocal, irregular, randomly distributed areas in all lung lobes (Cline et al. 2018). Additionally, as shown in the UMSOM studies, at four mo post WTLI, CT density correlated with elevated RR.

PE:TLV: Overall incidence of radiographic injury. The incidence of PE:TLV increased within 30 d after WTLI and ranged from 50% to 75% across all cohorts. The severity (volume) of PE was variable at any time point within each of the dose cohorts, as well as within cohorts of survivors and non-survivors. The PE resolved in the survivors within approximately 90 d post-irradiation and 120 d in non-survivors (Fig. 10b). Radiographically, the effusions in all cohorts were responsive to dexamethasone administration (Garofalo et al. 2014a).

WTLI and PBI/BM-sparing control cohorts: Comparative radiographic and clinical evidence of radiation-induced lung injury.

The continued definition of the natural history of RILI as evidenced by the time course of clinical, radiographic and histological indices is imperative to determining true effects of acute radiation exposure. The key dose- and time-dependent observations along longitudinal course of the ARS and DEARE identify the primary, secondary and tertiary endpoints and consequent triggers to administer medical management and organ-specific MCM. These include the latency or time from exposure to onset of manifestations of organ damage that include the longitudinal clinical and radiographic signs of morbidity and mortality. The comparative analysis of key parameters established a knowledge base to assess the evolution of the DEARE relative to potential impact of surviving the ARS as evidenced in database herein.

A comparative review of the radiographic data illustrated the concomitant time course of increased mortality, NSRR and radiographic indices of RILI, PF:TLV and PE:TLV by either PBI/BM-sparing or WTLI exposure protocols (Fig. 11a, b). Changes in mean NSRR for each cohort are plotted as a function of time post exposure. This analysis was restricted to the NHP data set that survived > 60 d post-exposure (e.g. survivors of GI-ARS and H-ARS coincident with prolonged GI) and for whom serial daily NSRR data were available. Animals were observed through the 180 d study duration.

All key parameters of the DEARE proceeded from a latent period of approximately 40 – 60 d followed by an increase in all three indices of clinical and radiographic evidence of RILI within the next 60 d to 120 d post exposure. The mean time to initiation of dexamethasone administration is relative to exposure protocol and radiation dose. This occurred at 98 d following both 11 Gy PBI/BM5 and 10 Gy PBI/BM2.5 and 127 d after 10 Gy PBI/BM5 (Table 4). Following WTLI at 10.74, 11, and 10 Gy, dexamethasone was initiated at 78 d, 90 d, and 117 d, respectively (Table 4). The subsequent time course and longitudinal analysis was influenced by the persistent progression of RILI, administration of dexamethasone and loss of NHP due to lethality. The modest number of evaluable NHP over the study duration influenced the statistical analysis.

Pneumonitis/fibrosis, PF:TLV, was evident as early as 30 d post 10 Gy exposure in both WTLI and PBI/BM protocols (Figs. 11a, b). The PF:TLV increased in all surviving NHP

throughout 120 d of the 180 d time course post exposure. Pleural effusion, PE:TLV: Pleural effusion was another CT-based parameter indicative of lung injury that had equivocal latency, incidence and apparent restricted duration relative to the other indices of lung injury in both, PBI/BM5 and WTLI exposure protocols. PE:TLV showed a marginal presence at 30 d followed by increased PE:TLV through 60 – 90 d post exposure. The incidence of PE appeared restricted to a time segment from 30 – 120 d post exposure. The incidence and severity of PE was likely influenced by administration of dexamethasone (MacVittie et al. 2012; Garofalo et al. 2014a; MacVittie et al. 2017; MacVittie et al. 2019a).

SUMMARY: Mortality, clinical and radiographic evidence of RILI: PF:TLV and PE:TLV relative to NSRR and mortality after PBI/BM-sparing and WTLI exposures.

A comparative review of the data illustrated the evolution of clinical (NSRR) and radiographic (PF:TLV, PE:TLV) evidence of RILI and mortality that proceeded from a latent period of approximately 40 – 60 d to a persistent level of incidence and severity that progressed within the 180 d study duration (Figs. 8–11). The subsequent time course and longitudinal analysis was influenced by the persistent progression of RILI, administration of dexamethasone and loss of NHP via euthanasia due to respiratory insufficiency. The modest number of evaluable NHP influenced statistical analysis, thereby providing evidence of trends relative to treatment and longitudinal effects relative to PBI/BM-sparing and WTLI exposure throughout the 180d study duration. *The evaluable database suggested that morbidity and mortality characteristic of acute RILI may be due to organ-specific systems focused in initiating RILI that may not be influenced by other concomitant organ sequelae that precede the overt incidence of lung injury. The equivalent latent period for RILI and DEARE-MOI evidenced within the PBI/BM-sparing and WTLI protocols may be defined by effects on biological systems that are independent of the early ARS-MOI and morbidity.*

Histopathological evidence of pneumopathy, “pneumonitis” and fibrosis.

PBI/BM-sparing and WTLI cohorts.—The CT-based radiodensity data did not permit differentiation of a “pneumonitic” or inflammatory stage from fibrosis. M-T and collagen-1 IHC staining was employed to identify the evaluable time course and incidence parameters relative to excessive collagen deposition indicative of fibrosis. The histological database supplied valuable longitudinal analysis and supportive data relative to the clinical and radiographic database associated with the time course of RILI (MacVittie et al. 2012; Garofalo et al. 2014a; MacVittie et al. 2019a; Parker et al. 2019c).

The initial analysis recorded signs of inflammation (pneumonitis), reflected in cellular infiltration, tissue damage and mediators to include identification of fibrosis, and multiple additional histological changes in all NHPs over the 180 d study duration. Acute radiation-induced pneumopathy, was defined herein by a confluence of clinical, radiographic and histological-based parameters. The histological evidence included longitudinal analysis of the morphological alteration of the lung that is discernible by imaging, gross necropsy inspection and routine histopathologic observation to include selective histochemical staining. The histological indices included alveolar edema, inflammatory cell infiltration, fibrosis, cellular proliferations and hyperplasia, selective staining with M-T, collagen-1, alpha SMA, etc.

PBI/BM-sparing control cohorts.—Pneumonitis, *per se was* based on histologic evidence of leukocytic/macrophage infiltrations with associated tissue alterations. This is the time-honored definition of inflammation from a pathologist's perspective. Fibrosis was based primarily on demonstration of fibrous connective tissue with M-T staining, with supporting indications from IHC staining for collagen 1 and alpha SMA.

Fibrosis.—Fibrosis was identified in both interstitial and pleural locations. The data showed a latency period of approximately 50 – 80 d post exposure in both tissue sites. The latent period is similar to that noted for the clinical and radiographic parameters of RILI. The histological grade of fibrosis remained elevated (grade range 2 – 4) and consistent throughout the 180 d duration. The fibrosis was predominant in the periphery of lobes whereas a significant cellular hyperplasia was noted more centrally near major airways. From a histopathological perspective, the fibrosis and hyperplasia appear to be unrelated pathologic events. Many of the lesions (fibrosis, etc.) were multifocal within the lung. Areas of pleural fibrosis tended to be associated with subjacent areas of interstitial fibrosis. Interstitial fibrosis, as revealed with M-T staining, was present sporadically in animals necropsied within 30 – 95 d and was present to some degree in all animals necropsied thereafter within the 180 d study duration. The trichrome stain also revealed focal or multifocal pleural fibrosis in animals necropsied on d 40 post-irradiation and thereafter (MacVittie et al. 2019a; Parker et al. 2019c).

Two different types of epithelial cell proliferation were observed. The most common change involved proliferation of type-2 pneumocytes, presumably in response to loss of type-1 pneumocytes. A common, proliferative change was distinctive alveolar-bronchiolar hyperplasia located near major airways.

WTLI cohorts.—Garofalo and colleagues reported histological data from 18 analyses, n = 3 at each dose cohort. The M-T staining from irradiated (11.0 Gy, WTLI) NHP lungs exhibited thickening of alveolar wall and diffuse fibrosis (Fig. 12 a-d) (Garofalo et al. 2014a). Fibrosis was increased when compared to the tissue sections from non-irradiated NHP. The average total percent positive for analine blue showed no DRR between radiation dose cohorts in sample analysis. This could be due to inconsistency of samples identified at necropsy as unaffected normal lung and damaged lung. The correlation between microscopic fibrosis to grossly observable damage at necropsy remained a confounding variable. The research team acknowledged the difficulty in using a histological analysis of lung damage such as trichrome staining to establish a quantitative value for the lung in a NHP model, given that we cannot analyze the whole lung due to size limitation. Additionally, the use of dexamethasone, as well as the fact that the dose delivered to the lung volume is nonuniform and likely is a major influence in the nonuniform, differential pathology (Prado et al. 2015; Prado et al. 2017). The histopathology is presented to show the temporal link between pneumonitis and fibrosis and the clinical and radiographic evidence of RILI.

Thrall and team indicated that histopathological correlation to prescribed radiation dose and time post exposure of a relatively large organ such as the lung was difficult. As noted earlier, the radiation dose gradient across the organ and administration of subject-based steroids, as well as the time post exposure, are confounding variables. Multiple tissue samples were

procured at each necropsy and analyzed via H&E and M-T staining (Thrall et al. 2019). The histological data confirmed the findings note by Garofalo and colleagues (Garofalo et al. 2014a). The most significant findings at 180 d were fibroplasias of the interstitium and pleura and macrophage infiltration of the interstitium (9.5 to 10.5 Gy). Less common findings included edema of the alveoli, mononuclear cell infiltration of the interstitium, hemorrhage of the alveoli, hypertrophy of the mesothelium of the pleura , mononuclear cell infiltration of the pleura, neutrophil infiltration of the alveoli (9.5 Gy), hyperplasia of the bronchiolar epithelium (9.5 and 10 Gy), and hyperplasia of type II pneumonocytes (9.5 and 10 Gy). Microscopic findings for unscheduled euthanasia included observations of myocardial degeneration of the heart.

Cline and colleagues summarized the affected regions of the lung in irradiated animals contained four major changes: (1) interstitial and intra-alveolar infiltration of the lung parenchyma by macrophages and other inflammatory cells, (2) accumulation of proteinaceous fluid in alveolar spaces, (3) hyperplasia and hypertrophy of alveolar lining cells, leading to the replacement of the normal thin oxygen exchange layer of type I pneumocytes with a thicker layer of cuboidal Type II cells, and (4) fibrosis of the pulmonary interstitium. Cline et al., stated that their findings in NHP exposed to 10 Gy WTLI were consistent with those of Garofalo et al., namely, in regard to progressive pneumonitis and pulmonary fibrosis, affecting all irradiated animals by four mo after radiation exposure (Garofalo et al. 2014a; Cline et al. 2018).

Summary: Acute radiation-induced lung injury; the time course of histopathology, NSRR and mortality.

A comparative review of the histopathological data derived from lung tissue at necropsy as well as the key clinical indices of NSRR illustrated the concomitant time course of mortality due to lung injury (Fig. 13a, b). The radiographic evidence of lung injury does not differentiate between pneumonitis and fibrosis. Thus, the key time and incidence parameters for the predominant histopathology in the lung such as fibrosis were identified by Masson's trichrome and collagen-1 IHC staining. Fibrosis was identified in both interstitial and pleural locations after a latency of approximate 50 – 80 d post exposure in either PBI/BM-sparing or WTLI cohorts (MacVittie et al. 2019a; Parker et al. 2019c). The severity or grade for fibrosis remained elevated (range 2 – 4) and consistent through the 180 d study duration. A similar latency period is noted for clinical and radiographic indices of lung injury. The NSRR in the PBI/BM-sparing cohorts increased slowly after the two mo latent period, to reach 60 bpm and then 80 bpm – the primary trigger for dexamethasone - after approximately 90 d and 100 d respectively post exposure and coincident with overt lung injury and mortality (Fig. 13b).

Tertiary studies and evidence-based support for PBI/BM-sparing and WTLI NHP models of RILI.

de Faria et al. (2015).—The pulmonary subsyndromes and cardiac effects are a pair of inter-dependent syndromes impacted by exposure to potentially lethal doses of radiation (van Luijk et al. 2005; Ghobadi et al. 2012b). Herein, de Faria and team demonstrated the use of CT and electrocardiographic data in the rhesus macaque PBI/BM-sparing and WTLI models to define: a) consistent and reliable methodology to assess radiation-induced

damage to the lung and heart, b) an extensive database in normal age-matched NHP for key primary and secondary endpoints, c) identified problematic variables in imaging techniques and proposed solutions to maintain data integrity and d) initiated longitudinal analysis of potentially lethal radiation-induced damage to the lung and heart in the NHP (de Faria et al. 2015). The MCART multi-modal imaging core was focused on exploring the potential of non-invasive imaging to perform longitudinal analysis of radiation-induced lung (pulmonary-DEARE) and heart (cardiac-DEARE) damage and assess MCM efficacy.

CT scans and echocardiograms were performed on 40 and 32, respectively, normal male rhesus macaques to establish baseline values. Of that number, 20 macaques were later used in longitudinal irradiation studies.

Making the connection between the lung and the heart.—The objective of this study was to observe and characterize the clinical and subclinical signs that characterized the lung and cardiac injury. Lung and heart co-irradiation is a known risk factor in developing tissue injury in the cardiopulmonary circuit (van Luijk et al. 2005; Ghobaldi et al. 2010; Ghobadi et al. 2012b). Radiographic and clinical evidence of lung injury may be observed as early as 30 d after irradiation and persisting through the 180 d study. However, the latent period for echocardiographic evidence of cardiac dysfunction appeared to be delayed until 90 d after irradiation, possibly an indication that the mechanisms causing cardiac damage are slower to develop.

Zhang et al. (2015).—The authors investigated the gene and protein expression of CTGF in multiple organs after exposure to lethal doses of radiation in two established NHP models - PBI/BM5 and WTLI - of radiation-induced fibrosis (Zhang et al. 2015). Organ tissues were procured from male Chinese rhesus macaques from contemporary studies performed at UMSOM. NHP were exposed to 9 – 12 Gy WTLI and 10 and 11 Gy PBI/BM5 with 6 MV LINAC-derived photons (MacVittie et al. 2012; Garofalo et al. 2014a; MacVittie et al. 2017). CTGF expression and collagen deposition were measured in the same organ. CTGF, a member of the CCN2 (cellular communication network factor 2) family of matricellular proteins, plays an important role in the development of fibrosis in multiple organs. Tissues from four to seven, age and bw-matched non-irradiated NHP and NHP exposed to WTLI or PBI/BM5 were examined by real-time quantitative reverse transcription polymerase chain reaction, western blot, and immunohistochemistry. Expression of CTGF was significantly elevated in the lung tissues of NHP exposed to WTLI within the time segments, 40 – 100 d and 100 – 165 d post 9.0 – 12.0 Gy. CTGF was expressed in multiple organs from NHP exposed to PBI/BM5 compared to non-irradiated NHP from 1 to 6 mo post 10 – 11 Gy exposure; these included the lung, kidney, spleen, thymus, and liver. The irradiated organs also exhibited histological evidence of increased collagen deposition compared to the control tissues. These data suggested that CTGF levels are increased in multiple organs after radiation exposure and that inflammatory cell infiltration may contribute to the elevated levels of CTGF.

Parker et al. (2019).—The goal was to determine the histopathological progress of radiation-induced and/or -associated alterations in the lung and heart of male rhesus macaques throughout the 180 d study duration post 10, 11 or 12 Gy with the UMSOM

PBI/BM5 protocol. (Parker et al. 2019c). In-life observations and clinical and radiographic parameters are described in companion publications (MacVittie et al. 2012; MacVittie et al. 2019a). NHP were euthanized within the study duration based on IACUC-criteria. Tissue sections from six normal NHP (mean age = 4.5 y) were used for comparison to the irradiated tissues.

Histological sections were stained with H&E and a battery of selected histochemical and IHC stains. Histopathological alterations in the lung were centered on fibrosis, inflammation and reactive/proliferative changes in pneumocytes in NHP necropsied from approximately 85 – 100 d to 180 d post exposure. Interstitial and pleural fibrosis (M-T) were associated with increased alpha SMA and collagen 1 IHC staining. Areas of interstitial fibrosis had reduced microvascular density (CD31) and an accumulation of CD163+ and CD206+ alveolar macrophages. Unidentified cells, termed “myxoid’ cells in alveolar walls had staining characteristics of epithelial-, endothelial-, or pericyte-mesenchymal transition states that were developing myofibroblast features. Histopathological changes in the heart consisted of myocardial fibrosis. Positive staining for alpha SMA was associated with myocardial fibrous connective tissue. The combination of observations suggested a radiation-associated increase in myofibroblast populations that promoted pulmonary fibrosis with persistent pathological processes due to expression of fibrogenic factors by proliferating pneumonocytes and alveolar macrophages. Tissue hypoxia may accentuate the pathology.

Carter et al. (2015).—Carter and colleagues initiated first mass spectrometry imaging (MSI) investigation into the spatial distribution of lipids within lung sections following irradiation of NHP within the UMSOM WTLI protocols. There is a significant gap in knowledge on the detection and spatial localization of specific lipid species during an active inflammatory response within the respiratory airways in irradiated NHP. The detection of lipids specific to immune infiltration within the alveolar space may prove pivotal in identifying new signaling molecules. WTLI of NHP induced persistent nuclear damage and gene expression changes in peripheral blood cells. The ability to localize specific lipid signatures to activated immune cells is of great importance as prolonged inflammatory insult following irradiation is believed to contribute to the onset of fibrosis. Additionally, the ability to map specific lipid species to distinct inflammatory cell accumulation for the given pathological presentation will enable us to construct a profile of markers reflective of the phenotype for injury severity, and resolution.

Carter et al. (2017).—Carter and colleagues utilized matrix-assisted laser desorption/ ionization (MALDI) - MSI to investigate lipidomic alterations within the differing lung pathologies detected at 180 days following high-dose, 10.74 Gy WTLI in rhesus macaques (Carter et al. 2017; MacVittie et al. 2017). Multiple lipids species were identified that showed alterations regardless of the pathological presentations following RILI, as well as molecules that correlated with inflammation and changes that reflect severe pulmonary fibrosis.

Lung biopsies residing next to those used for MSI were formalin fixed and paraffin embedded following standard clinical pathology protocols. Lung samples from naïve (non-

irradiated) and three different irradiated (d 180 post-radiation) NHP were formalin-inflated and embedded as previously described.

Lipids play central roles in metabolism and cell signaling, and thus reflect the phenotype of the tissue environment, making these molecules pivotal biomarkers in many disease processes. Decreases in specific surfactant lipids were detected, as well as regional increases in ether-linked phospholipids that are the precursors of platelet activating factor, and global decreases in lipids that were reflective of severe fibrosis. Taken together, results provided panels of lipids that can differentiate between naïve and irradiated samples, as well as providing potential markers of inflammation and fibrosis.

The reduction or loss in lipids within this lung region would have profound effects on the local lung physiology and provided evidence of a potential mechanism contributing to the severe impairment of cellular processes and lung function that are not solely attributed to collagen deposition. Combining highly sensitive analytical techniques with well-defined animal models enabled us to investigate local changes in diseased parenchyma, which is difficult in RILI as diseased lung can reside alongside normal appearing lung, and the nature of the disease is highly complex. Using MALDI-MSI to characterize the molecular changes that occur within regions of lung tissue during RILI has provided panels of lipids that can be used to reflect diseases state and have potential to serve as markers for injury in general.

Ghandhi et al. (2018).—Ghandhi and colleagues., investigated the cytogenetic and gene expression responses of peripheral blood cells of NHP (Macaca mulatta) that were exposed to a single 10 Gy of WTLI as per the exposure protocol described by Cline and colleagues (Cline et al. 2018). The team evaluated long-term DNA damage in peripheral blood lymphocytes via the cytokinesis-block micronucleus assay to assess chromosomal aberrations as post-mitotic micronuclei in blood samples collected up to 8 mo after irradiation. Regression analysis showed significant induction of micronuclei in NHP blood cells that persisted with a gradual decline over the 8 mo study period, suggesting long-term DNA damage in blood lymphocytes after WTLI. It was also reported that transcriptomic changes in blood were observed up to 30 d after WTLI. Total RNA was isolated from peripheral blood at 3 d before and then at 2, 5 and 30 d after irradiation. The changes in gene expression, 1187 transcripts, identified biological processes related to immune responses, which persisted across the 30-d study. Gene expression changes suggested a persistent altered state of the immune system, specifically response to infection, for at least one mo after WTLI.

SUMMARY: RILI consequent to PBI/BM-sparing or WTLI exposure protocols.

The key database and knowledge gaps addressed in the review herein were focused primarily on defining the comparable natural history between the PBI/BM-sparing and WTLI exposure protocols in the NHP. The effort focused on the comparative evolution of apparent equivalent, dose dependent RILI relative to the influence of potentially lethal ARS on the latency, incidence, severity and progression of RILI from the two markedly different exposure protocols. The key endpoints were the mortality dose response relationship and

clinical, radiographic and histopathological indices relative to their latency, incidence, severity and progression within the 180 d study duration.

The database: common variables; animals, radiation exposure, medical management, primary and secondary endpoints.

There were several common factors within the published primary, secondary and tertiary studies that worked to our advantage in marginalizing critical variables. These were: 1.) *Animals*. All NHP were rhesus macaques of Chinese origin, although with variable bw, UMSOM 5.3 – 10.4 kg, SNBL 4 – 6 kg and the Cline study 3.3 – 5.7 kg. The UMSOM and Cline studies used male and SNBL used female macaques (MacVittie et al. 2012; Garofalo et al. 2014a; MacVittie et al. 2017; Cline et al. 2018; MacVittie et al. 2019a; Thrall et al. 2019). 2.) *Radiation source and exposure parameters*. The review benefitted from the fact that all primary studies for both PBI/BM-sparing and WTLI protocols used approximate, AP/PA, uniform exposure of equivalent 6 MV LINAC-derived photons, delivered to the same target site, MLT at the xiphoid process, at dose rates that ranged from 0.80 – 2.00 Gy min^{-1} . The respective PBI/BM-sparing protocols exposed approximately 95 – 97.5% of the body with intended 5% and 2.5% BM sparing; the WTLI protocols exposed the whole thorax region with approximately the 35% of active BM located therein exposed (Taketa et al. 1970). 3.) D*ose distribution, the prescribed, descriptive dose relative to organ-specific dose*. The average dose to a specific organ volume will vary relative to the prescribed dose and target site, in this case, MLT at the xiphoid process. Prado et al., used three-dimensional dose calculations and tissue heterogeneity corrections to assess the respective dose to lung, kidney, heart consequent to relevant doses of both PBI/BM-sparing and WTLI used in the UMSOM NHP studies (Prado et al. 2015; Prado et al. 2017). The prescribed doses for the PBI/BM2.5 (10 Gy) and WTLI (10.74 Gy resulted in mean doses of 10.62 and 11.05 Gy to the lung volume. If warranted, the organ-specific pathology and mean organ dose could be linked to the prescribed and descriptive dose that defined the respective LD50/180 values. 4.) *Medical management and IACUC euthanasia criteria*. All NHP in the UMSOM, SNBL and Cline studies were administered medical management in accordance with IACUC-approved protocols that specified subject-based, clinical triggers-to-treat and stop. Dexamethasone was used in UMSOM and SNBL studies whereas prednisone was used in the Cline study (Garrison et al. 2009; MacVittie et al. 2012; Garofalo et al. 2014b; Cline et al. 2018; MacVittie et al. 2019a; Thrall et al. 2019). 5.) Primary and secondary study endpoints/parameters. The primary studies focused on four key dose- and time-dependent parameters, e.g., mortality, co-morbidities, clinical, radiographic and histopathological to define the time course of RILI and concomitant delayed MOI and the ARS MOI (MacVittie et al. 2012; Garofalo et al. 2014a; Cline et al. 2018; MacVittie et al. 2019a; Parker et al. 2019c; Thrall et al. 2019).

Conclusions and gaps in knowledge.

The dose- and time-dependent radiation-induced ARS, composed of the overt, acute hematopoietic (H)- and gastrointestinal (GI)-ARS and associated MOI to the kidney provided a foundation to approach the concurrent, latent and overt development of the DEARE and MOI. The MCART team and colleagues have focused on, a) developing a more strategic and integrated organ-based approach to determine radiation effects to single and

multiple organs characteristic of the ARS and DEARE, b) defining the efficacy of MCM administration in the context of MOI and c) the development of biomarker paradigms that will predict clinical outcome within the context of use.

Several questions were asked to initiate the review.

1. *What was the dose response relationship for all-cause mortality at a 180 d study duration for PBI/BM5 vs WTLI exposure*?

   The established NHP models of acute RILI at UMSOM used PBI/BM5, PBI/BM2.5 or WTLI exposure protocols whereas the SNBL team developed a WTLI protocol. The UMSOM and SNBL studies used male and female NHP, respectively. The DRR's were validated relative to their comparative LD values and slopes as well as a composite list of primary and secondary parameters that defined RILI in the male and female NHP. The parameters related to a modest, comparative human database (Prato et al. 1977; Fryer et al. 1978; Van Dyk et al. 1981). The DRR for mortality was comparable in the two predominant models using either PBI/BM5 or WTLI developed in male NHP or WTLI developed in male or female NHP (Fig.1a, b, c; Table 1). There was no significant difference between the LD50/180 values or the slopes of the DRR's between the PBI/BM5 or WTLI exposure protocols (P = 0.86). The respective LD50/180 values are 9.94 Gy and 10.24 Gy for respective studies at UMSOM. The respective LD50/180 values for the SNBL WTLI study in female NHP was 10.28 Gy. The respective slopes were approximate at 1.21, 1.15 and 1.72. NHP expressed RILI with comparable dose- and time-dependent, all-cause mortality assessed at the end of the 180d study duration consequent to PBI/BM-sparing or WTLI exposure protocols.

2. *What was the extent of the dose- and time-dependent MOI of the ARS in the PBI/BM-sparing models relative to WTLI?* The two exposure protocols, PBI/BM-sparing and WTLI, presented differential views of the time course that preceded the evolution of delayed MOI (Figs. 4 – 6). An initial approach centered on the assumption that the DRR for the DEARE, induced by the PBI/BM-sparing protocols would be markedly affected by the early co-morbidities and mortality due to the concomitant MOI of the ARS. The WTLI protocol was designed to focus on the lung (plus heart) and spare all the early sequelae associated with the ARS MOI as well as the chronic kidney injury and prolonged GI damage and thus present a model focused on acute irradiation of only the lung and heart.

   The early phase of morbidity and mortality noted within the longitudinal time course of the MOI within the ARS, reflected the influence of the concomitant GI- and H-ARS, AKI, immune suppression and co-morbidities on the longitudinal loss of survival probability in the PBI/BM-sparing models (Figs. 4 – 6, Tables 1– 3). The time course of mortality within the WTLI model was characterized by the early, relatively clinically silent latent period due to the sparing of high-dose exposure to the BM, GI and kidney and the absence of the overt ARS and associated co-morbidities. Thereafter, the continued loss

of survival probability was associated predominantly with overt lung injury in both models. The effects of differential, concomitant CKI, prolonged GI injury, immune suppression and heart injury in the respective models remain to be determined. *It is imperative to note that these overt signs of MOI in the ARS time course define the relatively silent or latent period prior to the overt evolution of MOI characteristic of the DEARE. A critical gap in knowledge was whether the overt signs during this latent period effect the incidence and time course of the DEARE.* Medhora and colleagues have shown a similar dose- and time-dependent DRR for RILI consequent to WTLI or PBI/BM-sparing in the WAG/RijCmcr rat model (Fish et al. 2016; Fish et al. 2020). The ARS MOI of the PBI/BM-sparing model was not an influence on morbidity and mortality of delayed lung and kidney mortality. Supportive evidence of disparate ARS and DEARE sequelae was also noted in a study comparing a subthreshold dose of TBI with marrow-sparing on delayed lung injury (Johnston et al. 2011).

3. *Was radiation-induced lung injury equivalent between the models, PBI/BM-sparing and WTLI?* The RILI was characterized by the dose-dependent mortality, clinical, radiographic and histological indices used to define the latency, incidence, severity and progression between PBI/BM-sparing and WTLI models.

   The latent period for RILI extended from approximately 1 to 40 d post exposure in both exposure and dose-equivalent protocols. The PBI/BM-sparing protocol was characterized by concomitant co-morbidities and organ-specific mortality and injury during this period due to the dose- and time-dependent MOI of the ARS. The time course for overt clinical, histological and radiographic incidence of RILI progressed from approximately 40 d through 180 d post exposure; the study duration for both PBI/BM-sparing and WTLI protocols.

   A comparative review of the data focused on cohorts of NHP exposed to 10 to11 Gy, PBI/BM-sparing and 10 to 11 Gy WTLI protocols. The database illustrated the concomitant time course of increased mortality and morbidity, and the clinical, radiographic and histological parameters. All key parameters proceeded from a latent period of approximately 40 – 60 d followed by an increase in all three indices of clinical, radiographic and histopathological evidence of RILI within the next 60 to 120 d that progressed through 180 d study duration. The subsequent time course and longitudinal analysis was influenced by the persistent progression of RILI, administration of dexamethasone and loss of NHP due to lethality. The modest number of evaluable NHP also influenced statistical analysis. *The database suggested that morbidity and mortality due to acute RILI and associated MOI may be due to organ-specific systems focused in initiating RILI that may be disparate and not influenced by other organ sequelae, the ARS MOI, that precede the overt incidence of lung injury and DEARE. The latent period for RILI and DEARE-MOI may be defined by effects on biological systems that are independent of the early ARS-MOI and morbidity.*

A comprehensive understanding of radiation effects, both acute and delayed, permits a study design for MCM efficacy to include consideration of current knowledge gaps such

as determining the effect of: a) an organ-specific MCM on other organ injury, b) combined MCM administration on MOI, c) MCM administration during the concomitant evolution of MOI within the ARS and DEARE, d) the effect of a consensus MCM with a mechanism of action for similar/equivalent sequelae (fibrosis) in multiple organs, e) clarify organ-specific radiation damage and recovery at critical trigger points for assessing administration of single and combination MCM efficacy, f) extending the study duration to permit adequate determination of the progression and resolution of the organ-specific injury in control and MCM-treated cohorts. Considerations relative to time of onset (latency), incidence, severity, progression, duration and resolution or durability of the sequelae are important to determine if the primary and secondary endpoints, such as key signs of morbidity and/or mortality are stabilized/resolved over the study duration (U. S. Food and Drug Administration 2015). We do not know the longitudinal extent of radiation-induced injury nor the true effect of MCM administration. g) Biomarkers: There are no reliable, validated biomarker paradigms that will predict organ-specific clinical outcome consequent to acute radiation exposure. h) ARS – DEARE causality: It Is not clear that the biological systems involved in the early ARS phase of high-dose radiation consequences using the PBI/BM5 exposure protocol are relevant to the initiation of the DEARE. Are the trigger-points required for the initiation of the latency, incidence, severity and progression of lung, kidney or heart injury influenced or set by systems affected during the ARS phase?

These are important considerations that will aid in defining prospective studies to assess the true treatment effect for MCM efficacy. It is beyond the scope of this review to consider the role of the complex cascade of cellular, humoral and molecular responses triggered by threshold doses of radiation that result in acute and delayed MOI and fibrosis. The database herein suggested that the radiation-induced activation of the “inflammasome” may be involved in initiating disparate pathways for the time- and dose-dependent MOI of the ARS and the DEARE.

This database suggested that morbidity and mortality consequent to acute RILI may be due to organ-specific systems focused in initiating RILI that may not be influenced by other concomitant organ sequelae consequent to the ARS that precede the overt incidence of lung injury. The latent period for RILI and DEARE-MOI may be defined by effects on biological systems that are independent of the early ARS-MOI and morbidity.

Acknowledgments

This project has been funded in whole or in part with federal funds from the National Institute of Allergy and Infectious Diseases, National Institute of Health under contracts HHSN272201000046C, SRI/NIAID Contract HHSN272201500013I and from Aeolus Inc. through BARDA contract HHSO100201100007C.

References

Asano S. Multi-organ involvement: lessons from the experience of one victim of the Tokai-mura criticality accident. Br J Radiol 78; 2005.

Baranov AE, Selidovkin GD, Butturini A, Gale RP. Hematopoietic recovery after 10-Gy acute total body radiation. Blood 83: 596–599; 1994. [PubMed: 8286754]

Berkely FJ. Managing the adverse effects of radiation therapy. AM Fam Physician 82: 381–388; 2010. [PubMed: 20704169]

Boittin F-X, Martigne P, Mayol J-F, Denis J, Raffin F, Coulon D, Grenier N, Drouet M, Herodin F. Experimental quantification of delayed radiation-indduced organ damage in highly irradiated rats with bone marrow protection: effect of radiation dose and organ sensitivity. Health Phys 109: 134–144; 2015. [PubMed: 26107434]

Carter CL, Jones JW, Farese AM, MacVittie TJ, Kane MA. Lipidomic dysregulation within the lung parenchyma following whole-thorax lung irradiation: Markers of injury, inflammation and fibrosis detected by MALDI-MSI. Sci Rep 7: 10343; 2017. [PubMed: 28871103]

Cline JM, Dugan G, Bourland JD, Perry DL, Stitzel JD, Weaver AA, Jiang C, Tovmasyan A, Owzar K, Spasojevic I, Batinic-Haberle I, Vujaskovic Z. Post-Irradiation Treatment with a Superoxide Dismutase Mimic, MnTnHex-2-PyP(5+), Mitigates Radiation Injury in the Lungs of Non-Human Primates after Whole-Thorax Exposure to Ionizing Radiation. Antioxidants (Basel) 7; 2018.

Cohen EP, Hankey KG, Bennett AW, Farese AM, Parker GA, MacVittie TJ. Acute and chronic kidney injury in a non-human primate model of partial-body irradiation with bone marrow sparing. Radiat Res 188: 661–671; 2017. [PubMed: 29035153]

Cohen EP, Hankey KG, Farese AM, Parker GA, Jones J, Kane MA, Bennett A, MacVittie TJ. Radiation nephropathy in a nonhuman primate model of partial-body irradiation with minimal bone marrow sparing. Part 1: acute and chronic kidney injury and the influence of Neupogen. Health Phys 116: 401–4008; 2019. [PubMed: 30608245]

Cui W, Bennett AW, Zhang P, Barrow KR, Kearney SR, Hankey KG, Taylor-Howell C, Gibbs AM, Smith CP, MacVittie TJ. A non-human primate model of radiation-induced cachexia. Sci Rep 6: 23612; 2016. [PubMed: 27029502]

Dainiak N, Gent RN, Carr Z, Schneider R, Bader J, Buglova E, Chao N, Coleman CN, Ganser A, Gorin C, Hauer-Jensen M, Huff LA, Lillis-Hearne P, Maekawa K, Nemhauser J, Powles R, Schunemann H, Shapiro A, Stenke L, Valverde N, Weinstock D, White D, Albanese J, Meineke V. First global consensus for evidence-based management of the hematopoietic syndrome resulting from exposure to ionizing radiation. Disaster med public health prep 5: 202–212; 2011a. [PubMed: 21987000]

Dainiak N, Gent RN, Carr Z, Schneider R, Bader J, Buglova E, Chao N, Coleman CN, Ganser A, Gorin C, Hauer-Jensen M, Huff LA, Lillis-Hearne P, Maekawa K, Nemhauser J, Powles R, Schunemann H, Shapiro A, Stenke L, Valverde N, Weinstock D, White D, Albanese J, Meineke V. Literature review and global consensus on management of acute radiation syndrome affecting nonhematopoietic organ systems. Disaster medicine and public health preparedness 5: 183–201; 2011b. [PubMed: 21986999]

de Faria EB, Barrow K, Ruehle BT, Parker JT, Swartz E, Taylor-Howell C, Kieta KM, Lees C, Sleeper MM, Dobbin T, Baron AD, Mohindra P, MacVittie TJ. The evolving MCART multimodal imaging core: Establishing a protocol for computed tomography and echocardiography in the rhesus macaque to perform longitudinal analysis of radiation-induced organ injury. Health Phys 109: 479–492; 2015. [PubMed: 26425907]

DeBo RJ, Lees CJ, Dugan GO, Caudell DL, Michalson KT, Hanbury DB, Kavanagh K, Cline JM, Register TC. Late Effects of Total-Body Gamma Irradiation on Cardiac Structure and Function in Male Rhesus Macaques. Radiat Res 186: 55–64; 2016. [PubMed: 27333082]

Farese AM, Bennett AW, Gibbs AM, Hankey KG, Prado K, Jackson III W, MacVittie TJ. Efficacy of Neulasta or Neupogen on H- and GI-ARS mortality and hematopoietic recovery in nonhuman primates after 10 Gy irradiation with 2.5% bone marrow sparing. Health Phys 116: 339–353; 2019. [PubMed: 30281533]

Farese AM, Cohen MV, Katz BP, Smith CP, Jackson W III, Cohen DM, MacVittie TJ. A nonhuman primate model of the hematopoietic acute radiation syndrome plus medical management. Health Phys 103: 367–382; 2012. [PubMed: 22929469]

Faubel S. Pulmonary complications after acute kidney injury. Advances in chronic kidney disease 15: 284–96; 2008. [PubMed: 18565479]

Faubel S, Edelstein CL. Mechanisms and mediators of lung injury after acute kidney injury. Nature reviews Nephrology 12: 48–60; 2016. [PubMed: 26434402]

Finney DJ. Probit Analysis:A statistical treatment of the sigmoid response curve In: City: Cambridge University Press; Year: 256.

Fish BL, Gao F, Narayanan J, Bergom C, Jacobs ER, Cohen EP, Moulder JE, Orschell CM, Medhora M. Combined hydration and antibiotics with lisinopril to mitigate acute and delayed high-dose radiation injuries to multiple organs. Health Phys 111: 410–419; 2016. [PubMed: 27682899]

Fish BL, MacVittie TJ, Szabo A, Moulder JE, Medhora M. WAG/RijCmcr rat models for injuries to multiple organs by single high dose ionizing radiation: similarities to nonhuman primates (NHP). Int J Radiat Biol 96: 81–92; 2020. [PubMed: 30575429]

Fryer CJH, Fitzpatrick PJ, Rider WD, Poon P. Radiation pneumonitis: experience following a large single dose of radiation. Int J Radiation Oncology 4: 931–936; 1978.

Garofalo M, Bennett A, Farese AM, Harper J, Ward A, Taylor-Howell C, Cui W, Gibbs A, Lasio G, Jackson W 3rd, MacVittie TJ. The delayed pulmonary syndrome following acute high-dose irradiation: a rhesus macaque model. Health Phys 106: 56–72; 2014a. [PubMed: 24276550]

Garofalo MC, Ward AA, Farese AM, Bennett A, Taylor-Howell C, Cui W, Gibbs A, Prado KL, MacVittie TJ. A pilot study in rhesus macaques to assess the treatment efficacy of a small molecular weight catalytic metalloporphyrin antioxidant (AEOL 10150) in mitigating radiation-induced lung damage. Health Phys 106: 73–83; 2014b. [PubMed: 24276551]

Garrison AP, Helmrath MA, Dehaney CM. Intestinal Stem Cells. Journal of Pediatric Gastroenterology and Nutrition 49: 2–7; 2009. [PubMed: 19502994]

Ghobadi G, Bartelds B, van der Veen SJ, Dickinson MG, Brandenburg S, Berger RMF, Langendijk JA, Coppes RP, van Luijk P. Lung irradiation induces pulmonary vascular remodeling resembling pulmonary artierial hypertension. Thorax 67: 334–341; 2012a. [PubMed: 22201162]

Ghobadi G, van der Veen S, Bartelds B, de Boer RA, Dickinson MG, de Jong JR, Faber H, Niemantsverdriet M, Brandenburg S, Berger RFM, langendijk M, Coppes RP, van Luijk P. Physiological interaction of heart and lung in thoracic irradiation. Int'l J Radiat Oncol Biol and Physics 84: e639–e646; 2012b.

Ghobaldi G, Hogeweg LE., Faber H, Tukker WG, Schippers JM, Brandenburg S, Langendijk JA, Coppes RP, van Luijk P. Quantifying local radiation-induced lung damage from computed tomography. Int J Radiat Oncol Biol Phys 76: 548–556; 2010. [PubMed: 20117290]

Gross NJ. Radiation pneumonitis in mice. Some effects of corticosteroids on mortality and pulmonary physiology. J Clin Invest 66: 504–510; 1980. [PubMed: 7400326]

Gross NJ, Narine KR, Wade R. Protective effect of corticosteroids on radiation pneumonitis in mice. Radiat Res 113: 112–119; 1988. [PubMed: 3340715]

Guskova AK, Nadezhina N, Barabanova AV, Baranov AE, Gusev IA, Protasova TG, Boguslavskij VB, Pokrovskaya VN. Acute effects of radiation exposure following the Chernobyl acident, Immediate results of radiation sickness and outcome of treatment. In: Browne D, Weiss JF, MacVittie TJ, Pillais MV eds. Treatment of Radiation Injuries New York: Plenum Press; 1990; 195–209.

Hsia CCW, Ravikumar P, Ye J. Acute lung injury complicating acute kidney injury: A model of endogenous alphaKlotho deficiency and distant organ dysfunction. Bone 100: 100–109; 2017. [PubMed: 28347910]

Jacobs ER, Narayanan J, Fish BL, Gao F, Harmann LM, Bergom C, Gasperetti T, Strande JL, Medhora M. Cardiac remodeling and reversible pulmonary hypertension during pneumonitis in rats after 13-Gy partial-body irradiation with minimal bone marrow sparing: Effect of lisinopril. Health Phys 116: 558–565; 2019. [PubMed: 30624347]

Johnston CJ, Manning C, Hernady E, Reed C, Thurston SW, Finkelstein JN, Williams JP. Effect of total body irradiation on late lung effects: hidden dangers. Int J Radiat Biol 87: 902–13; 2011. [PubMed: 21574903]

Kazi AM, MacVittie TJ, Lasio G, Lu W, Prado KL. The MCART radiation physics core: The quest for radiation dosimetry standardization. Health Phys 106: 97–105; 2014. [PubMed: 24276553]

Mackarehtschian K, Hardin JD, Moore KA, Boast S, Goff SP, Lemischka IR. Targeted disruption of the *flk2/flt3* gene leads to deficiencies in primitive hematopoietic progenitors. Immunity 3: 147–161; 1995. [PubMed: 7621074]

MacVittie TJ, Bennett A, Booth C, Garofalo M, Tudor G, Ward A, Shea-Donohue T, Gelfond D, Mcfarland E, Jackson W III, Lu W, Farese AM. The prolonged gastrointestinal syndrome in rhesus macaques: the relationship between gastrointestinal, hematopoietic, and delayed multi-organ

sequelae following acute, potentially lethal, partial-body irradiation. Health Phys 103: 427–453; 2012. [PubMed: 22929471]

MacVittie TJ, Bennett AW, Cohen V, Farese AM, Higgins A, Hankey KG. Immune cell reconstitution after exposure to potentially lethal doses of radiation in the nonhuman primate. Health Phys 106: 84–96; 2014. [PubMed: 24276552]

MacVittie TJ, Bennett AW, Farese AM, Taylor-Howell C, Smith CP, Gibbs AM, Prado K, Tudor G, Booth C, Jackson WI. The effect of radiation dose and variation in Neupogen® initiation schedule on the mitigation of myelosuppression during the concomitant GI-ARS and H-ARS in a nonhuman primate model of high-dose exposure with marrow sparing. Health Phys 109: 427–439; 2015. [PubMed: 26425903]

MacVittie TJ, Farese AM, Parker GA, Jackson III W. The time course of radiation-induced lung injury in a nonhuman primate model of partial-body irradiation with minimal bone marrow sparing: Clinical and radiographic evidence and the effect of Neupogen administration. Health Phys 116: 366–382; 2019a. [PubMed: 30624350]

MacVittie TJ, Farese AM, Parker GA, Jackson III W, Booth C, Tudor GL, Hankey KG, Potten C. The gastrointestinal syndrome of the acute radiation syndrome in rhesus macaques: A systematic review of the lethal dose response relationship with and without medical management. Health Phys 116: 305–338; 2019b. [PubMed: 30624353]

MacVittie TJ, Gibbs A, Farese AM, Barrow K, Taylor-Howell C, Bennett A, Kazi A, Prado K, Jackson WI. AEOL 10150 mitigates radiation-induced lung injury in the nonhuman primate: Morbidity and mortality are administration schedule-dependent. Radiat Res 187: 298–318; 2017. [PubMed: 28208025]

Mahmood J, Jelveh S, Zaidi A, Doctrow SR, Hill RP. Mitigation of radiation-induced lung injury with EUK-207 and genistein: effects in adolescent rats. Radiat Res 179: 125–34; 2013. [PubMed: 23237541]

Medhora M, Gao F, Glisch C, Narayanan J, Sharma A, Harmann LM, Lawlor MW, Snyder LA, Fish BL, Down JD, Moulder JE, Strande JL, Jacobs ER. Whole-thorax irradiation induces hypoxic respiratory failure, pleural effusions and cardiac remodeling. J Radiat Res 56: 248–60; 2015. [PubMed: 25368342]

Parker GA, Cohen EP, Li N, Takayama K, Farese AM, MacVittie TJ. Radiation nephropathy in a nonhuman primate model of partial-body irradiation with minimal bone marrow sparing-Part 2: Histopathology, mediators, and mechanisms. Health Phys 116: 409–425; 2019a. [PubMed: 30624348]

Parker GA, Li N, Takayama K, Booth C, Tudor GL, Farese AM, MacVittie TJ. Histological features of the development of intestine and mesenteric lymph node injury in a nonhuman primate model of partial-body irradiation with minimal bone marrow sparing. Health Physics 116: 426–446; 2019b. [PubMed: 30624355]

Parker GA, Li N, Takayama K, Farese AM, MacVittie TJ. Lung and heart injury in a nonhuman primate model of partial-body irradiation with minimal bone marrow sparing: Histopathological evidence of lung and heart injury. Health Phys 116: 383–400; 2019c. [PubMed: 30688698]

Phillips TL, Wharam MD, Margolis LW. Modification of radiation injury to normal tissues by chemotherapeutic agents. Cancer 35: 1678–1684; 1975. [PubMed: 50122]

Prado C, Kazi A, Bennett AW, MacVittie TJ, Prado K. Mean organ doses resulting from non-human primate whole thorax lung irradiation prescribed to mid-line tissue. Health Phys 109: 367–373; 2015. [PubMed: 26425898]

Prado C, MacVittie TJ, Bennet AW, Kazi A, Farese AM, Prado K. Organ doses associated with partial-body irradiation with 2.5% bone-marrow sparing of the non-human primate: A retrospective study. Radiat Res 188: 615–625; 2017. [PubMed: 28985133]

Prato FS, Kurdyak R, Saibil EA, Carruthers JS, Rider WD, Aspin N. The incidence of radiation pneumonitis as a result of single fraction upper half body irradiation. Cancer 39: 71–78; 1977. [PubMed: 832253]

Taketa ST, Carsten AL, Cohn SH, Atkins HL, Bond VP. Active bone marrow distribution in the monkey. Life Sci 9: 169–174; 1970. [PubMed: 4985006]

Thrall KD, Mahendra S, Jackson MK, Jackson W III, Farese AM, MacVittie TJ. A comparative dose response relationship (DRR) between genders for mortality and morbidity of radiation-induced lung injury in rhesus macaque. Health Phys 116: 354–365; 2019. [PubMed: 30688697]

U. S. Food and Drug Administration. New Drug and Biological Drug Products; Evidence Needed to Demonstrate Effectiveness of New Drugs When Human Efficacy Studies Are Not Ethical or Feasible 67: 37988–37998; 2002. Available at: https://www.govinfo.gov/content/pkg/FR-2002-05-31/pdf/02-13583.pdf Accessed 6/16/2020

U. S. Food and Drug Administration. Guidance for Industry: Product Development Under the Animal Rule [online] Washington, DC: U.S. Department of Health and Human Services, Center for Drug Evaluation and Research (CDER), and Center for Biologics Evaluation and Research (CEBR); 2015 Available at: http://www.fda.gov/downloads/drugs/guidancecomplianceregulatoryinformation/guidances/ucm399217.pdf. Accessed 06/16/2020.

Uozaki H, Fukayama M, Nakagawa K, Ishikawa T, Misawa S, Doi M, Maekawa K. The pathology of multi-organ involvement: two autopsy cases from the Tokai-mura criticality accident. BJR Suppl 27: 13–16; 2005.

van Bekkum DW. Radiation sensitivity of the hemopoietic stem cell. Radiat Res 128: S4–8; 1991. [PubMed: 1924746]

Van Dyk J, Keane TJ, Kan S, Rider WD, Fryer CJ. Radiation pneumonitis following large single dose irradiation: a re-evaluation based on absolute dose to lung. Int J Radiat Oncol Biol Phys 7: 461–467; 1981. [PubMed: 7251416]

van Luijk P, Novakova-Jiresova A, Faber H, Schippers JM, Kampinga HH, Meertens H, Coppes RP. Radiation damage to the heart enhances early radiation-induced lung function loss. Cancer Res 65: 6509–6511; 2005. [PubMed: 16061627]

Zhang P, Cui W, Hankey KG, Gibbs A, Smith C, Taylor-Howell C, Kearney S, MacVittie TJ. Increased expression of connective tissue growth factor (CTGF) in multiple organs after exposure of non-human primates (NHP) to lethal doses of radiation. Health Phys 109: 374–390; 2015. [PubMed: 26425899]

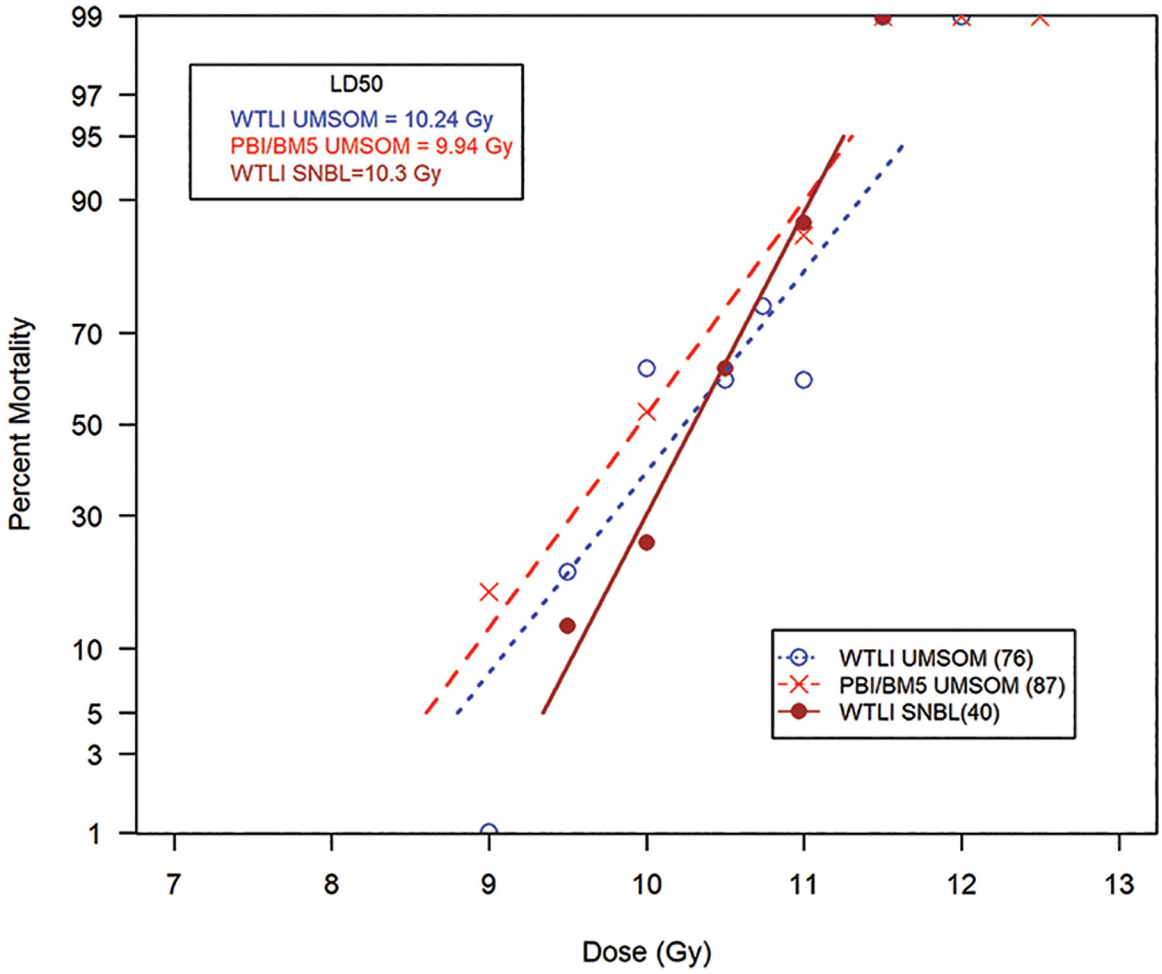

Fig. 1. Dose response relationship (DRR) for radiation-induced lung injury induced by partial-body irradiation with approximately 5% bone marrow sparing (PBI/BM5) or whole thorax lung irradiation (WTLI) exposure protocols in rhesus macaques.

UMSOM protocols. Rhesus macaques, male, were exposed to 6 MV LINAC-derived photons delivered to prescribed dose at midline tissue (xiphoid process) at a dose rate of 0.80 Gy min^{-1}. *SNBL protocols*. Female macaques were exposed to 6 MV LINAC-derived photons delivered to prescribed dose at midline tissue at 1.0 ± 0.05 Gy min^{-1}. All NHP received subject-based medical management as per respective IACUC-approved criteria and shared protocols. The DRRs were defined over time frames to assess organ-specific sub-syndromes over the 180 d study duration to assess radiation-induced lung injury characteristic of the DEARE. Irradiation protocols and exposures of WTLI (10.24 Gy) and PBI/BM5 (9.94 Gy) and WTLI (10.3 Gy) conducted at UMSOM and SNBL are compared.

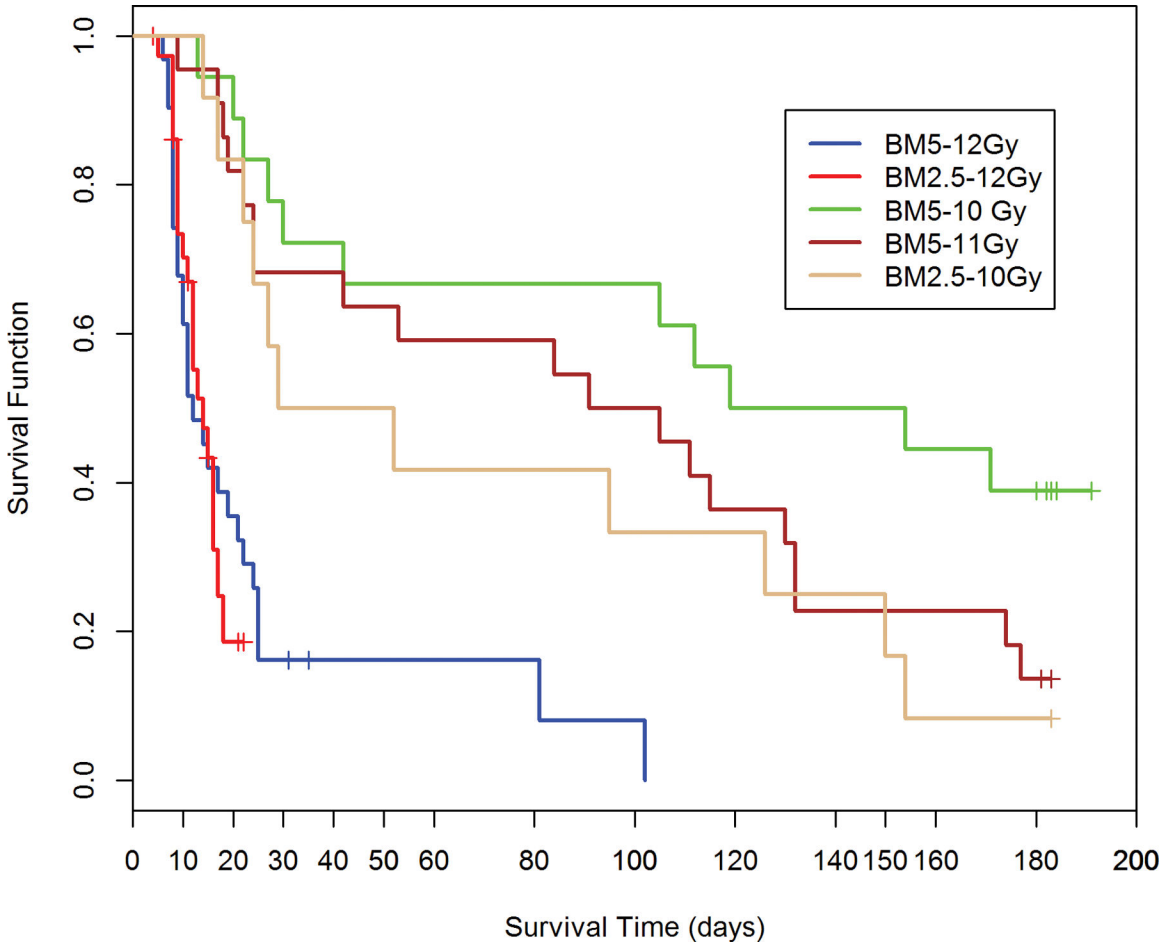

Fig. 2. Kaplan-Meier plot of survival probability demonstrating time-, dose- and protocol-dependent outcome relative to two exposure protocols in rhesus macaques.

Nonhuman primates at the UMSOM research site were exposed to uniform 6 MV LINAC-derived photons at a dose rate of 0.80 Gy min^{-1}. All prescribed exposures were measured at midline tissue dose (xiphoid process). Animals received IACUC-approved, subject-based medical management to include dexamethasone. Two exposure protocols were used, PBI/BM5 and PBI/BM2.5, three doses of radiation and differential BM-sparing using PBI/BM5 10 Gy and 11 Gy or PBI/BM2.5 at 10 Gy or 12 Gy (PBI/BM2.5) or 12 Gy (PBI/BM5) respectively. A clear survival effect is noted between 10 and 11Gy using the PBI/BM5 protocol and between the PBI/BM5 and PBI/BM2.5 protocols at 10Gy.

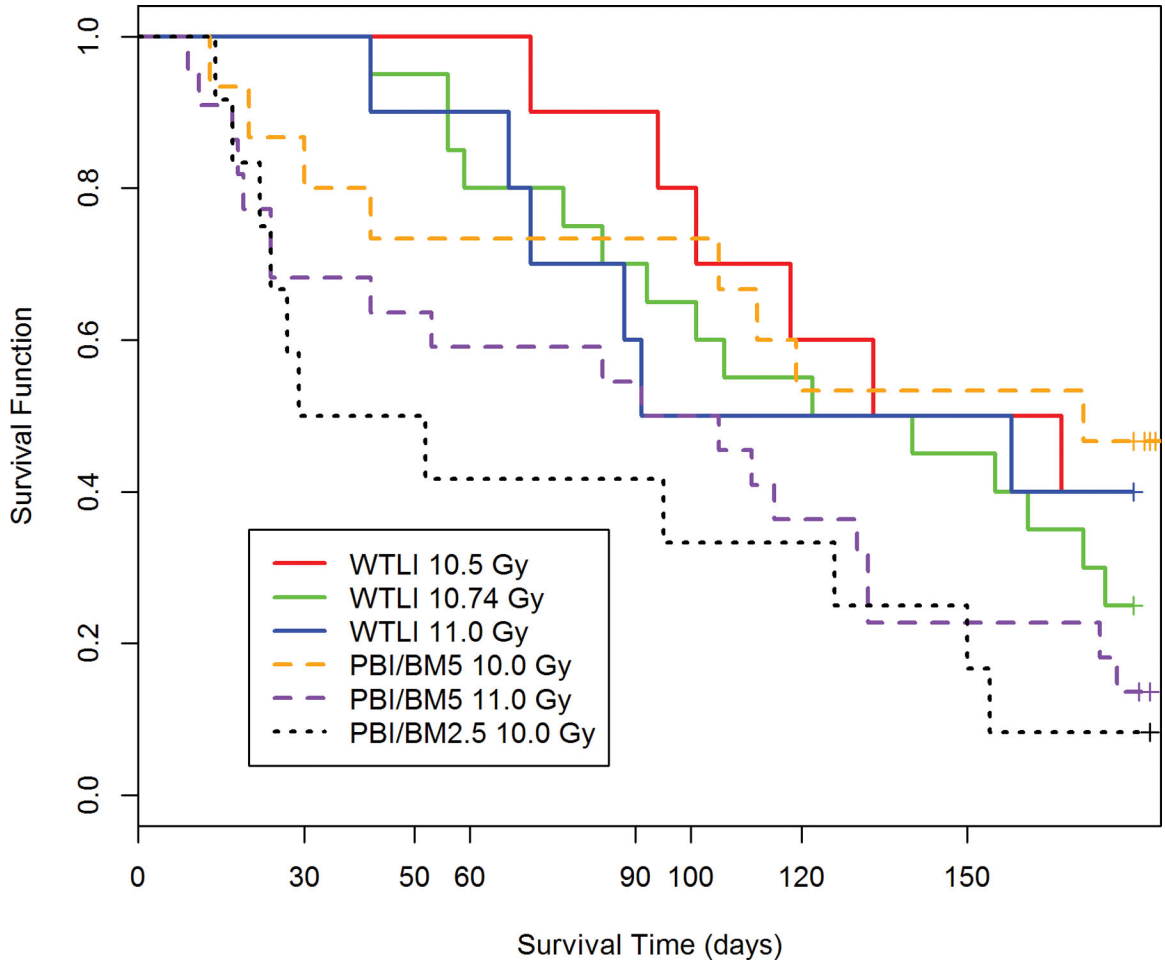

Fig. 3. Kaplan-Meier survival curves for rhesus macaque studies using the WTLI or PBI/BM2.5, PBI/BM5 exposure protocols: Relative all-cause mortality or survival probability over the 180 d study duration.

Nonhuman primates at the UMSOM research site were exposed to uniform 6 MV LINAC-derived photons at a dose rate of 0.80 Gy min^{-1}. All prescribed exposures were measured at midline tissue dose (xiphoid process). Animals received IACUC-approved, subject-based medical management to include dexamethasone. Nonhuman primates were exposed to 10.5 Gy (n = 10), 10.74 Gy (n = 20) or 11 Gy (n = 10) using the WTLI protocol or 10 Gy (n = 15) or 11 Gy (n = 21) using the PBI/BM5 protocol or 10 Gy (n = 12) using the PBI/BM2.5 protocol at the UMSOM research site. Euthanasia was performed based on IACUC-defined criteria.

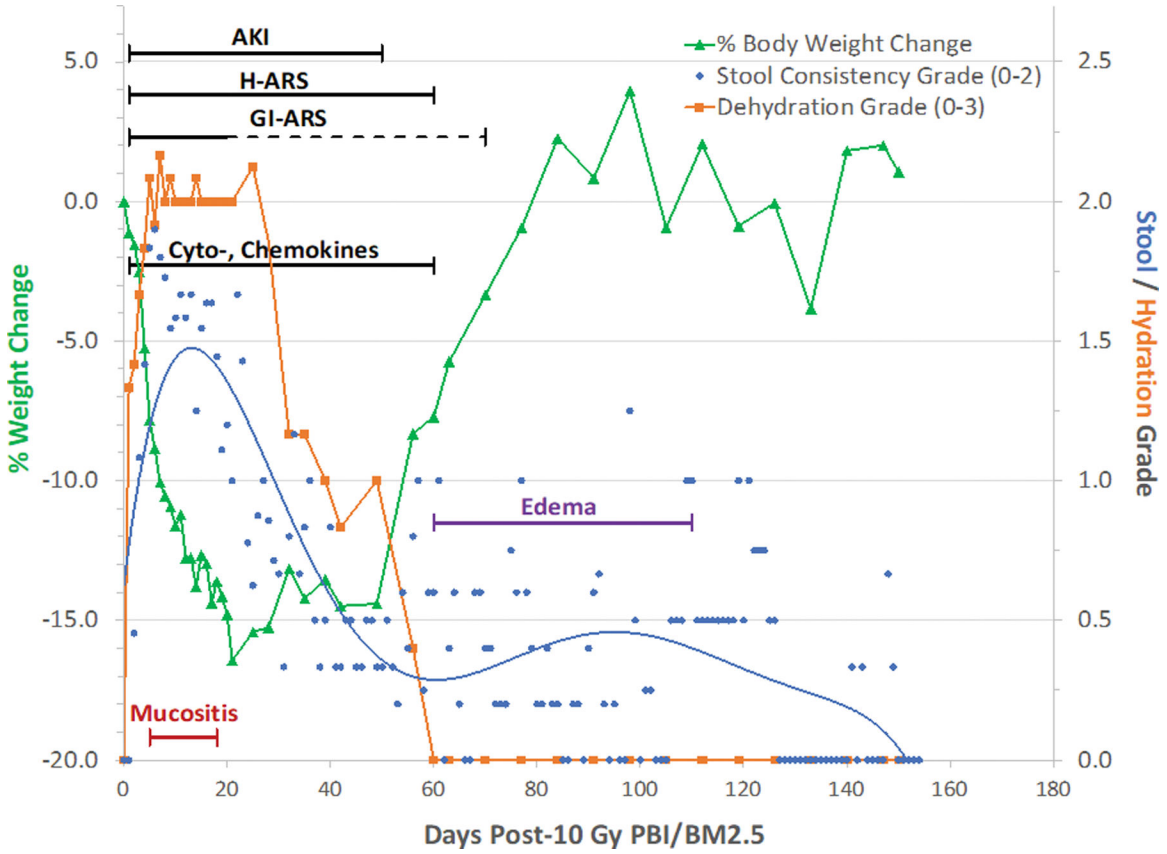

Fig. 4. PBI/BM-sparing, the ARS-MOI time segment: The multi-organ ARS and clinical signs for NHP consequent to 10 Gy PBI/BM-sparing protocol.

Rhesus macaques were exposed to 10 Gy partial body irradiation with approximately 2.5% bone marrow sparing (PBI/BM2.5) by 6 MV LINAC-derived photons delivered to prescribed dose at midline tissue (xiphoid process) at a dose rate of 0.80 Gy min^{-1}. Animals received IACUC-approved, subject-based medical management to include dexamethasone. The early clinical signs, to include dehydration, diarrhea, loss of body weight, cachexia, mucositis, plasma-based mediators and late occurring edema occur in the context of the overt multiple organ injury (MOI) characteristic of the acute radiation syndrome (ARS), e.g., GI-, H-ARS plus GI damage, immune suppression and acute kidney injury (AKI). The “early phase” clinical signs are presented in the context of the 180 d study duration. The time segment of the ARS represents the relatively “silent”, two mo latent period for MOI characteristic of the delayed effects of the acute radiation exposure (DEARE). The delayed edema and overt DEARE are evident at approximately 60 – 80 d post exposure (MacVittie et al. 2012; Farese et al. 2019).

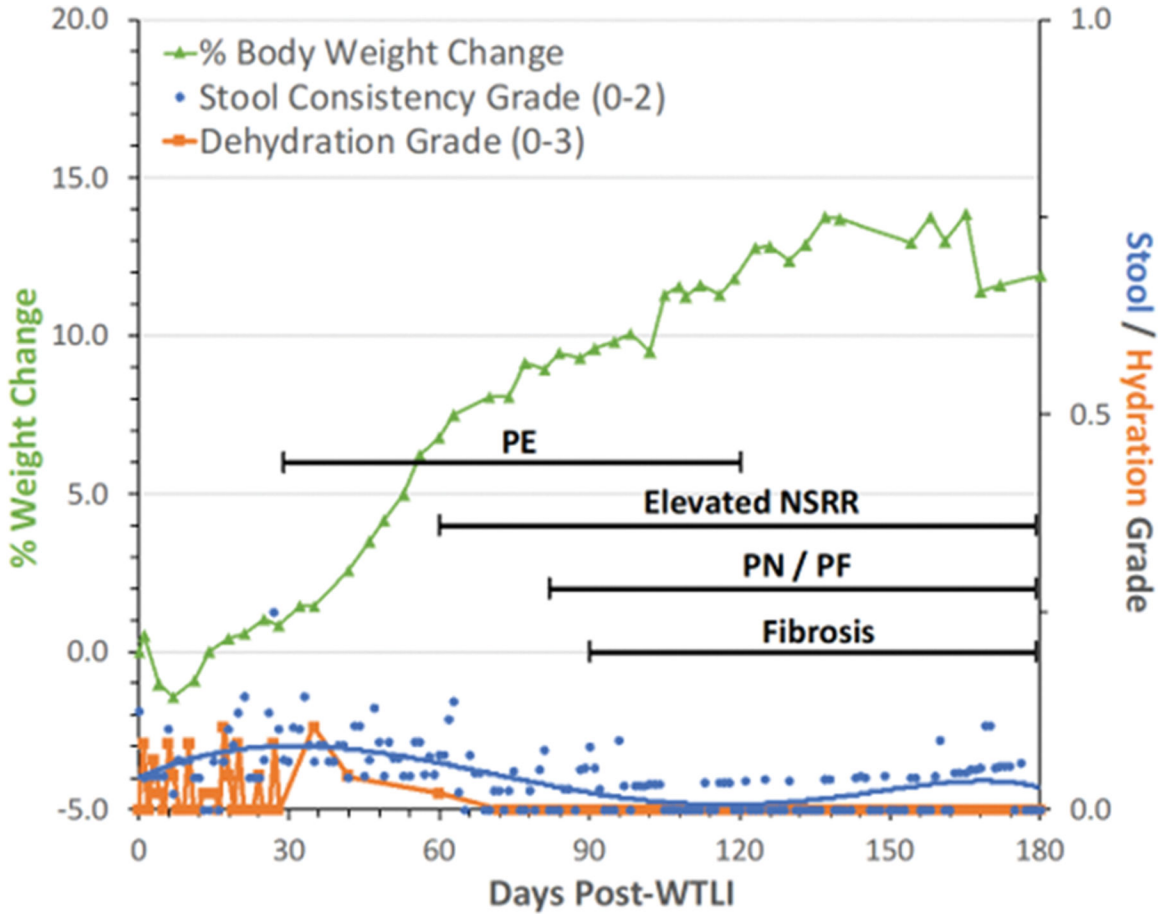

Fig. 5. The DEARE MOI time segment: The multi-organ injury within the DEARE and clinical signs for NHP consequent to 10 Gy – 11 Gy exposure using the WTLI protocol.

Rhesus macaques were exposed to 10 to 11 Gy whole thorax lung irradiation (WTLI), by 6 MV LINAC-derived photons delivered to prescribed dose at midline tissue (xiphoid process) at a dose rate of 0.80 Gy min^{-1}. Animals received IACUC-approved, subject-based medical management to include dexamethasone. Lack of severe clinical signs noted in the "early phase" of the PBI/BM-sparing models is also evident in the context of the 180 d study duration after WTLI. The early time segment, 1 – 40 d, also represents the relatively "silent" or latent period for multiple organ injury (MOI) characteristic of the delayed effects of the acute radiation exposure (DEARE). The DEARE are characterized by lung-associated pleural effusion (PE), pneumonitis/fibrosis (PN/PF), (F) fibrosis and increased non-sedated respiratory rate (NSRR). The DEARE includes a prolonged and skewed repertoire of memory and naïve subsets of immune suppression since the thymus is within the WTLI field (Garofalo et al. 2014a; Garofalo et al. 2014b; MacVittie et al. 2014; MacVittie et al. 2017).

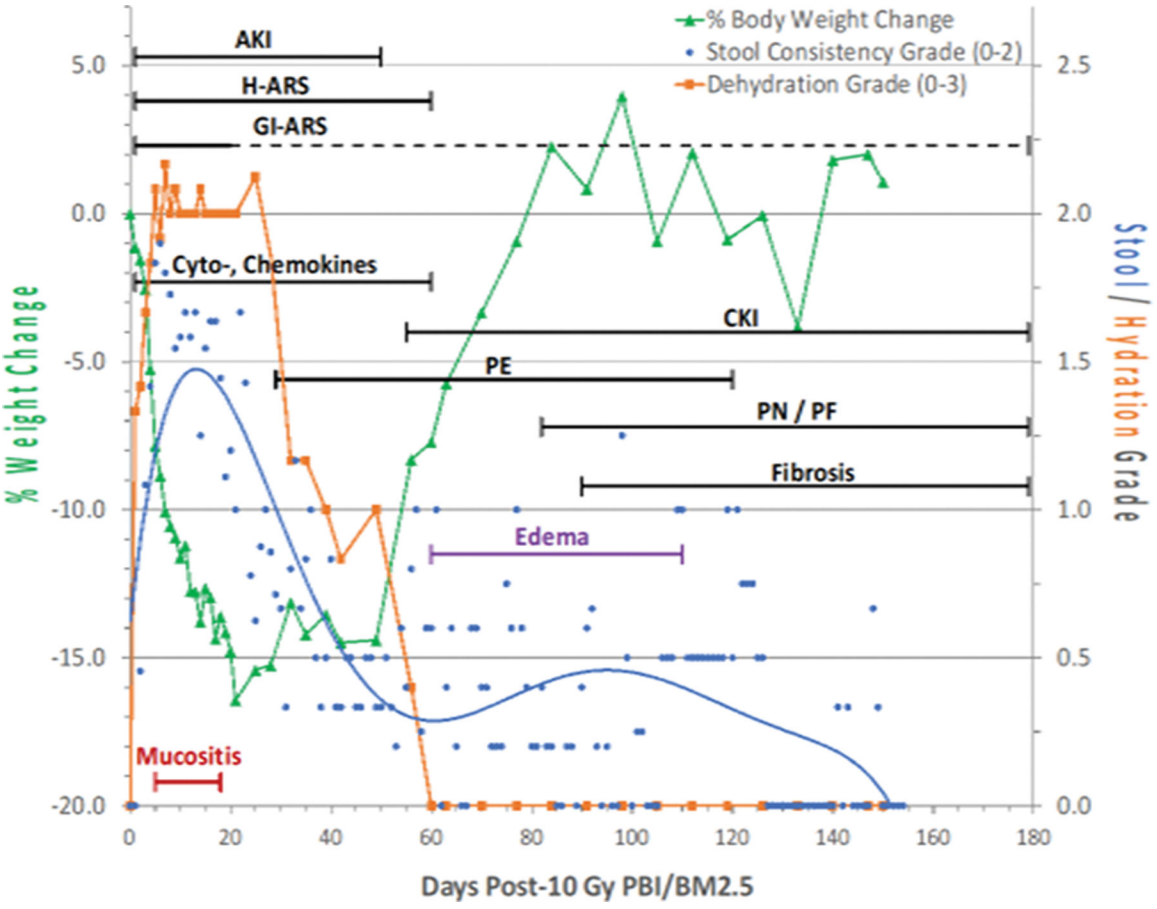

Fig. 6. The ARS-DEARE time segment: The multi-organ injury within the ARS and DEARE and clinical signs for NHP consequent to 10 Gy PBI/BM2.5 exposure protocol.

Nonhuman primates at the UMSOM research site were exposed to 10 Gy partial-body irradiation with approximately 2.5% bone marrow sparing (PBI/BM2.5) by uniform 6 MV LINAC-derived photons at a dose rate of 0.80 Gy min^{-1}. All prescribed exposures were measured at midline tissue dose (xiphoid process). Animals received IACUC-approved, subject-based medical management to include dexamethasone. The early clinical signs, to include dehydration, diarrhea, loss of body weight, cachexia, mucositis, plasma-based mediators and late occurring edema occur in the context of the overt multiple organ injury (MOI) characteristic of the acute radiation syndrome (ARS), e.g., GI-, H-ARS plus GI damage, immune suppression and acute kidney injury (AKI). The “early phase” clinical signs are presented in the context of the 180 d study duration. The early time segment also represents the relatively “silent”, two mo latent period for MOI characteristic of the delayed effects of the acute radiation exposure (DEARE). The DEARE are characterized by lung-associated pleural effusion (PE), pneumonitis/fibrosis (PF), fibrosis (F) and chronic kidney injury (CKI). The DEARE also include prolonged GI injury and a skewed repertoire of memory and naïve subsets of immune suppression. The delayed edema as overt DEARE was evident at approximately 60 – 80 d post exposure (MacVittie et al. 2014; Farese et al. 2019; MacVittie et al. 2019a).

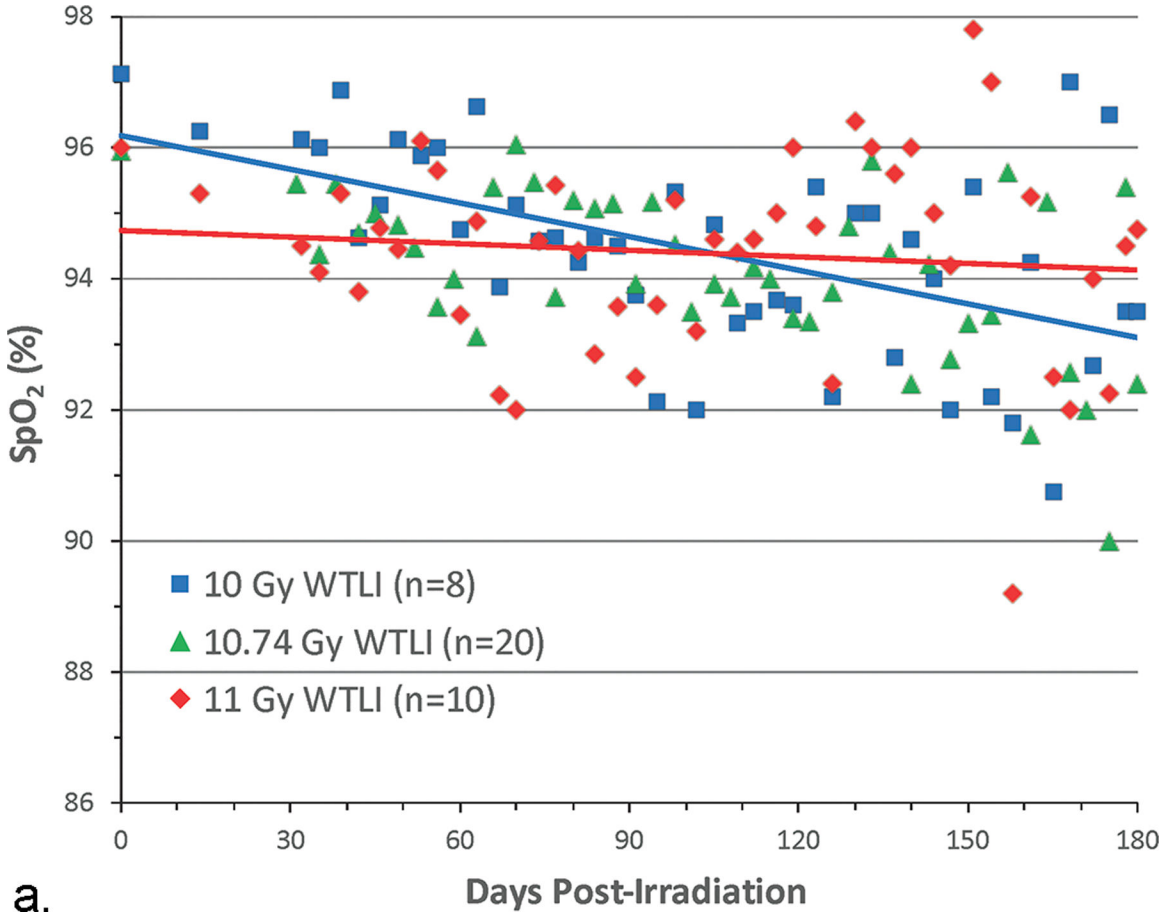

a.

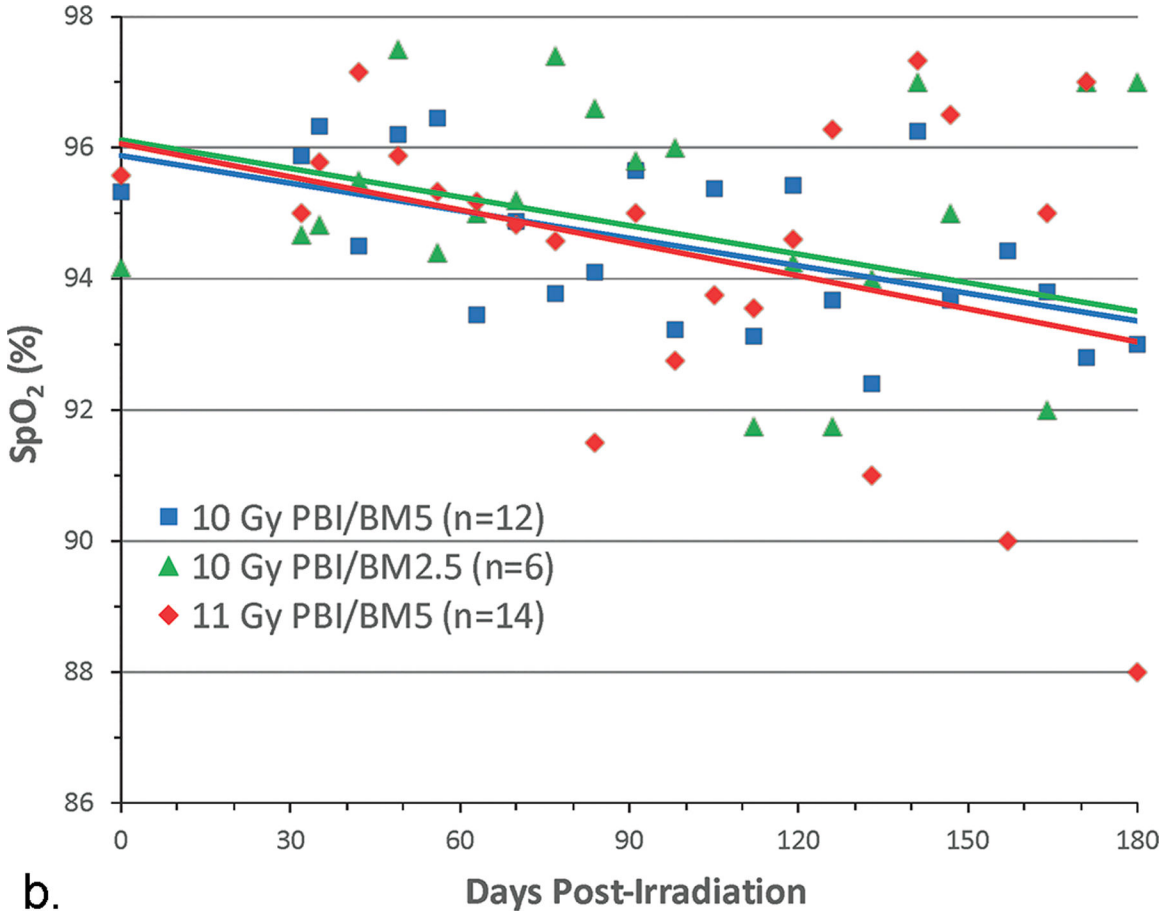

Fig. 7. Pulse oximetry, SpO_2 values: Comparison, using a "best fit" line of mean SpO_2 values over time post exposure for cohorts of NHP exposed to WTLI and PBI/BM-sparing protocols.

Rhesus macaques were exposed at 10 to 11 Gy, 6 MV LINAC-derived photons delivered to prescribed dose at midline tissue (xiphoid process) at a dose rate of 0.80 Gy min^{-1} to (a) whole thorax lung irradiation (WTLI) and (b) partial body irradiation with approximately 2.5% or 5% bone marrow sparing (PBI/BM). Animals received IACUC-approved, subject-based medical management to include dexamethasone. The oxygen saturation (SpO_2) values are a measure of compensated respiratory function over the 180 d study duration (MacVittie et al. 2012; Garofalo et al. 2014a; MacVittie et al. 2017).

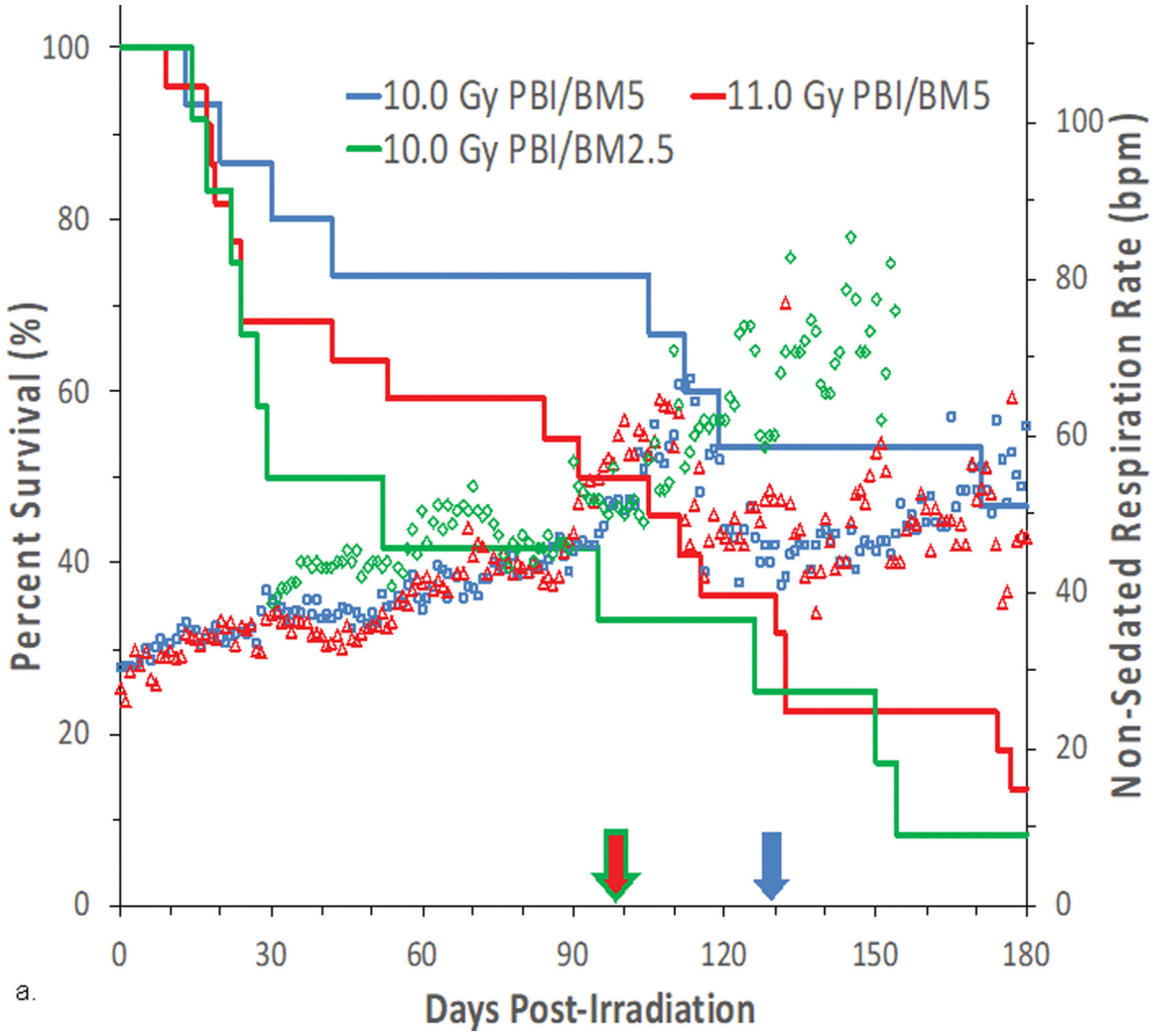

a.

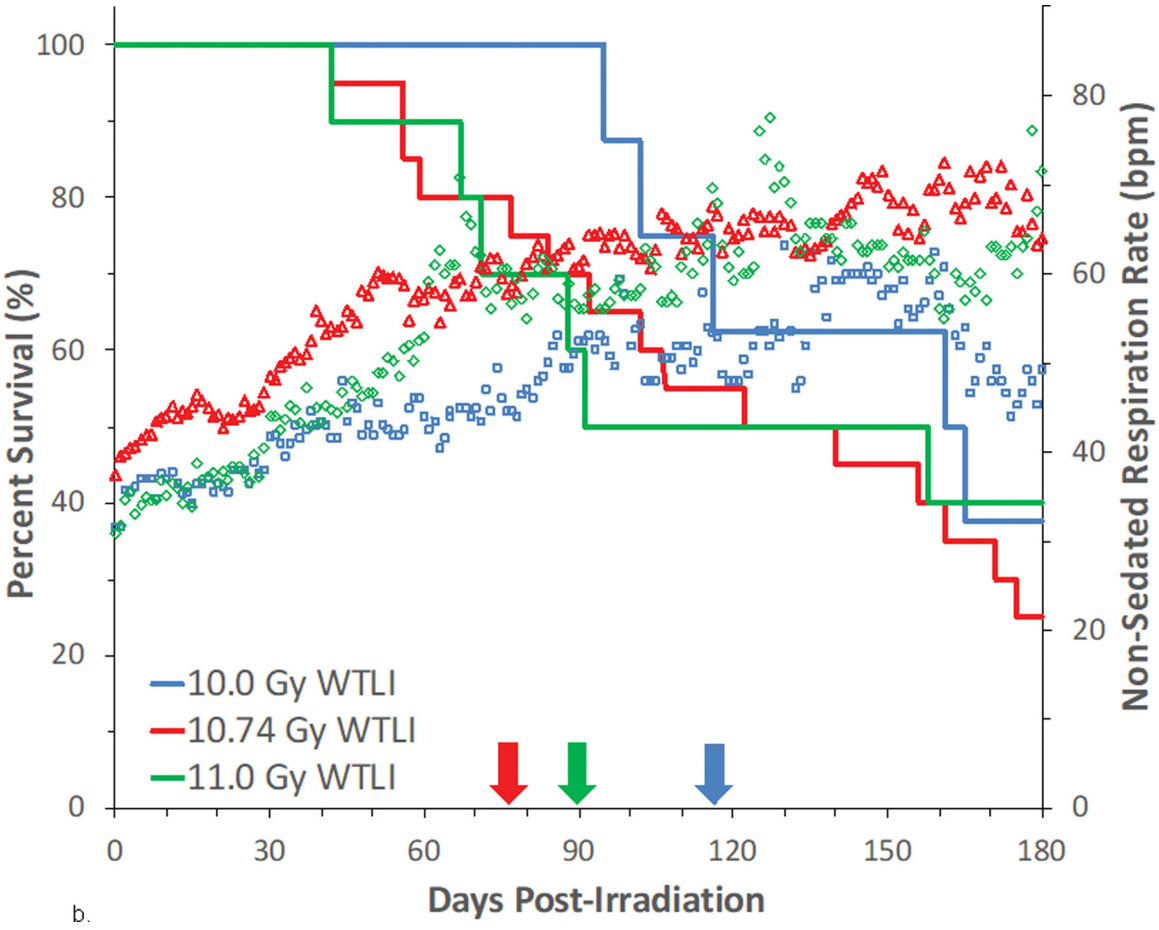

Fig. 8. Kaplan-Meier survival curves for a) the PBI/BM-sparing exposure protocols and b) the WTLI exposure protocol: Relative mortality/survival probability and non-sedated respiratory rate (NSRR).

Rhesus macaques were exposed to (a) 10 to 11 Gy partial body irradiation (PBI) with approximately 2.5% or 5% bone marrow (BM) sparing, or (b) 10 to 11 Gy whole thorax lung irradiation (WTLI) by 6 MV LINAC-derived photons delivered to prescribed dose at midline tissue (xiphoid process) at a dose rate of 0.80 Gy min^{-1}. Animals were observed through the 180d study duration. Animals received IACUC-approved, subject-based medical management to include dexamethasone. Changes in mean NSRR for each cohort are plotted as a function of time post exposure. This analysis was restricted to the NHP data sets that survived > 60 days post-exposure (e.g. survivors of GI-ARS and H-ARS coincident with prolonged GI) and for whom serial daily NSRR data were available. The mean time (d) to initiation of dexamethasone administration is color-coded relative to radiation dose and exposure protocol: 11 Gy PBI/BM5 (98), 10 Gy PBI/BM2.5 (98) and 10 Gy PBI/BM5 (127); WTLI at 10.74 Gy (78), 11 Gy (90), and 10 Gy (117d).

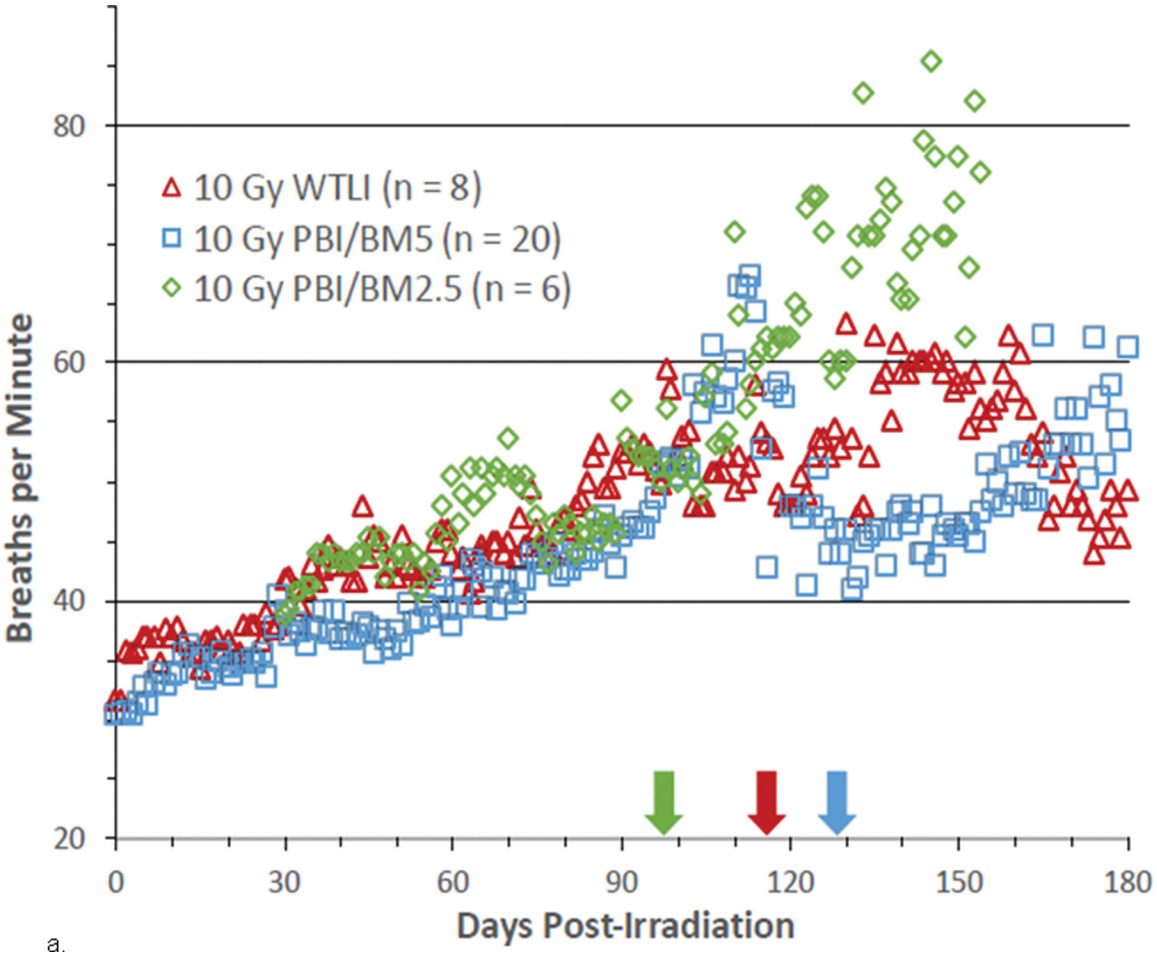

a.

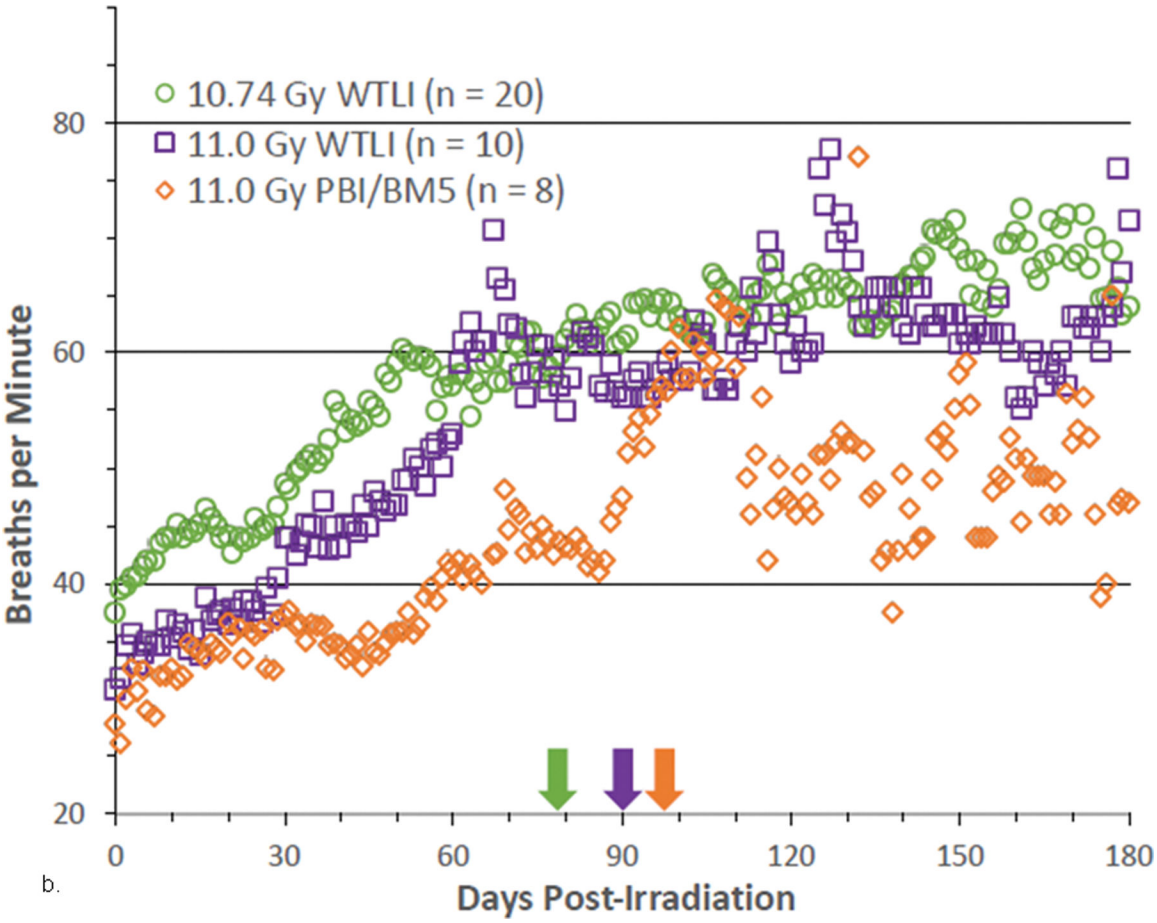

Fig. 9. NSRR measured as breaths per minute in NHP exposed to PBI/BM-sparing and WTLI protocols.

Rhesus macaques were exposed at 10 to 11 Gy, 6 MV LINAC-derived photons delivered to prescribed dose at midline tissue (xiphoid process) at a dose rate of 0.80 Gy min^{-1} to either whole thorax lung irradiation (WTLI) or approximately 2.5% or 5% bone marrow sparing (PBI/BM). Animals received IACUC-approved, subject-based medical management to include dexamethasone. Changes in mean non-sedated respiratory rate (NSRR) are plotted as a function of time post irradiation. Cohorts are from contemporary sequential studies that included model development for PBI/BM5 and WTLI and those assessing the efficacy of a proprietary medical countermeasure. The analysis was restricted to NHPs that survive > 60 d post exposure. The mean first day of dexamethasone administration for each cohort are delineated by color-coded arrows: (a) WTLI 10 Gy (117 d), 10 Gy PBI/BM5 (127.7 d) and 10 Gy PBI/BM2.5 (98.4 d), and (b) 10.74 Gy WTLI (78 d), 11.0 Gy WTLI (90 d), and 11 Gy PBI/BM5 (98 d).

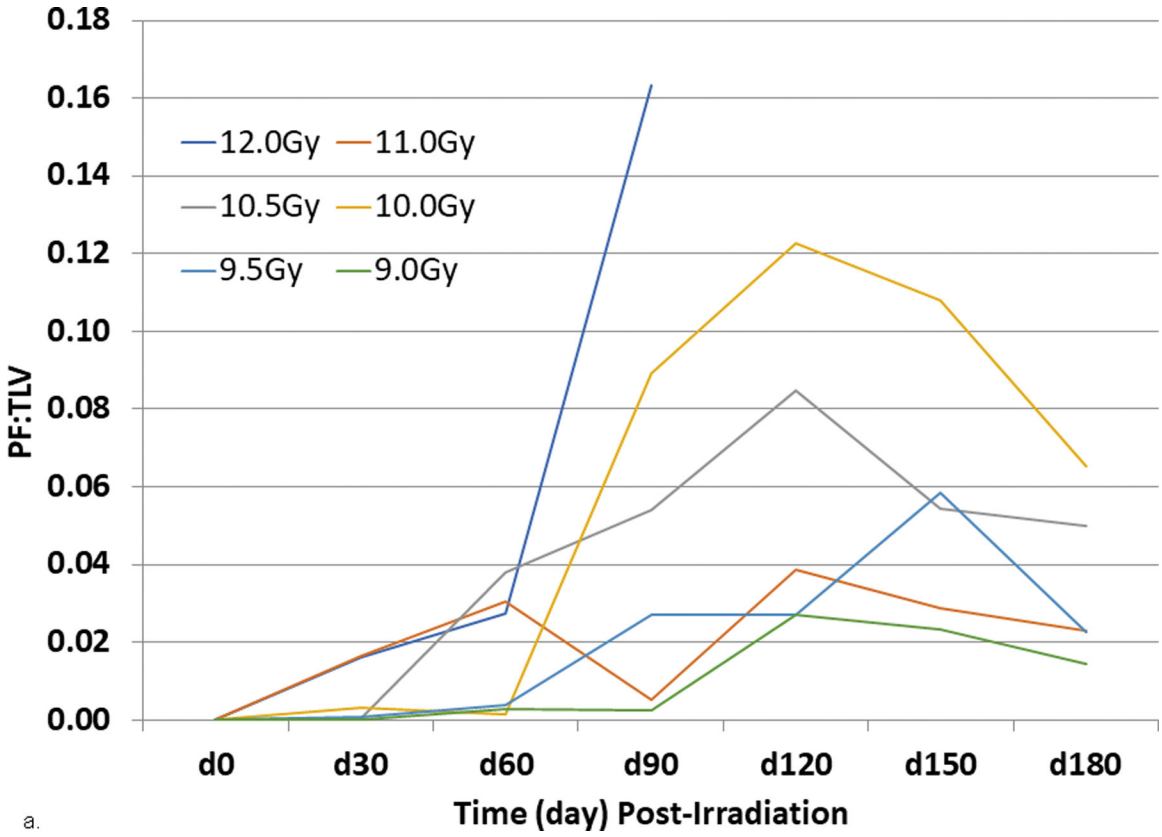

a.

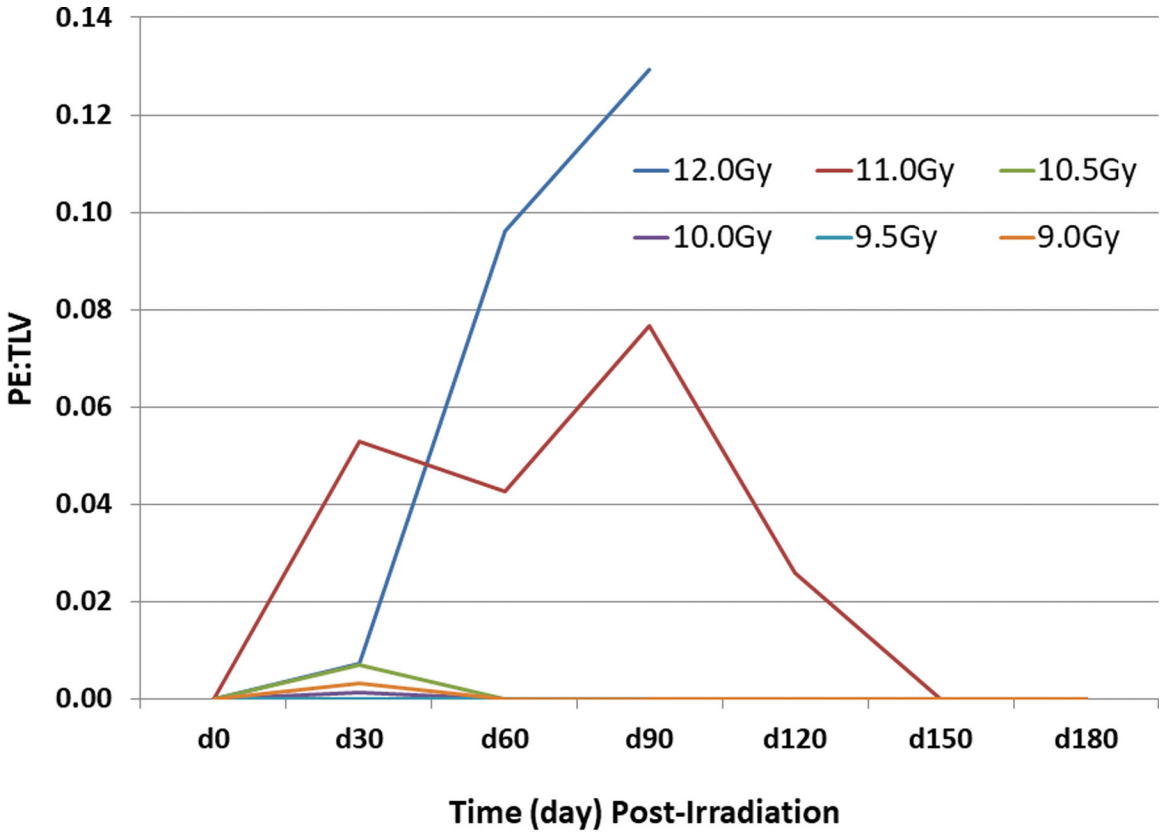

b.

Fig. 10. Radiographic analysis pneumonitis/fibrosis relative to total lung volume (PF:TLV) in NHP exposed to WTLI.

Rhesus macaques were exposed at 9 to 12 Gy whole thorax lung irradiation (WTLI), by 6 MV LINAC-derived photons delivered to prescribed dose at midline tissue (xiphoid process) at a dose rate of 0.80 Gy min^{-1}. Radiographic analysis of lung injury by computed tomography (CT), showing (a) the mean ratio of volume of pneumonitis and fibrosis indexed against the total lung volume (PF:TLV) or (b) the mean ratio of volume of pleural effusion (PE) indexed against the total lung volume (PE:TLV) as a function of exposure dose and time post-exposure. CT scans were performed at baseline and every 30 days post-exposure until the end of study or until the animal was euthanized for cause. Subject-based dexamethasone administration and ongoing lethality of nonhuman primates (NHP) with greatest pulmonary injury influences the results present beyond d 30 (Garofalo et al. 2014a).

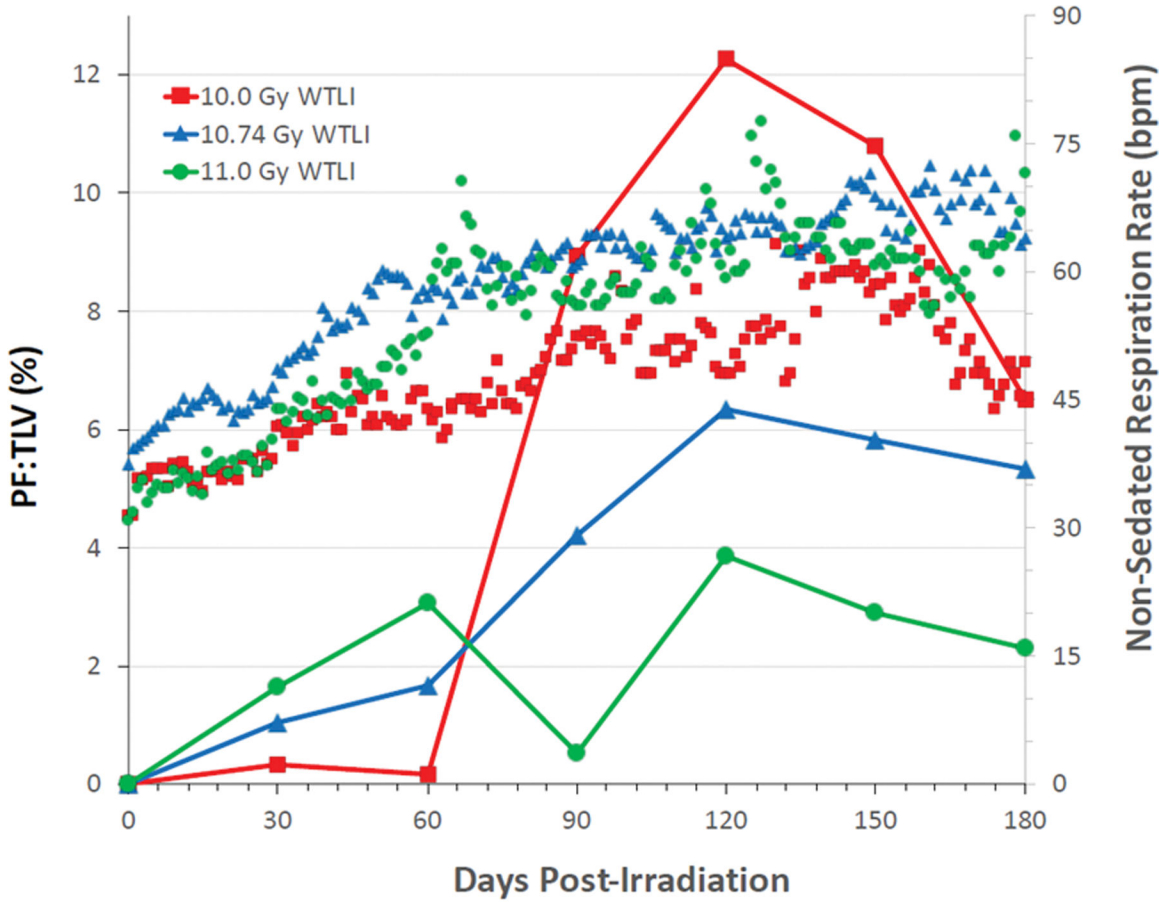

a.

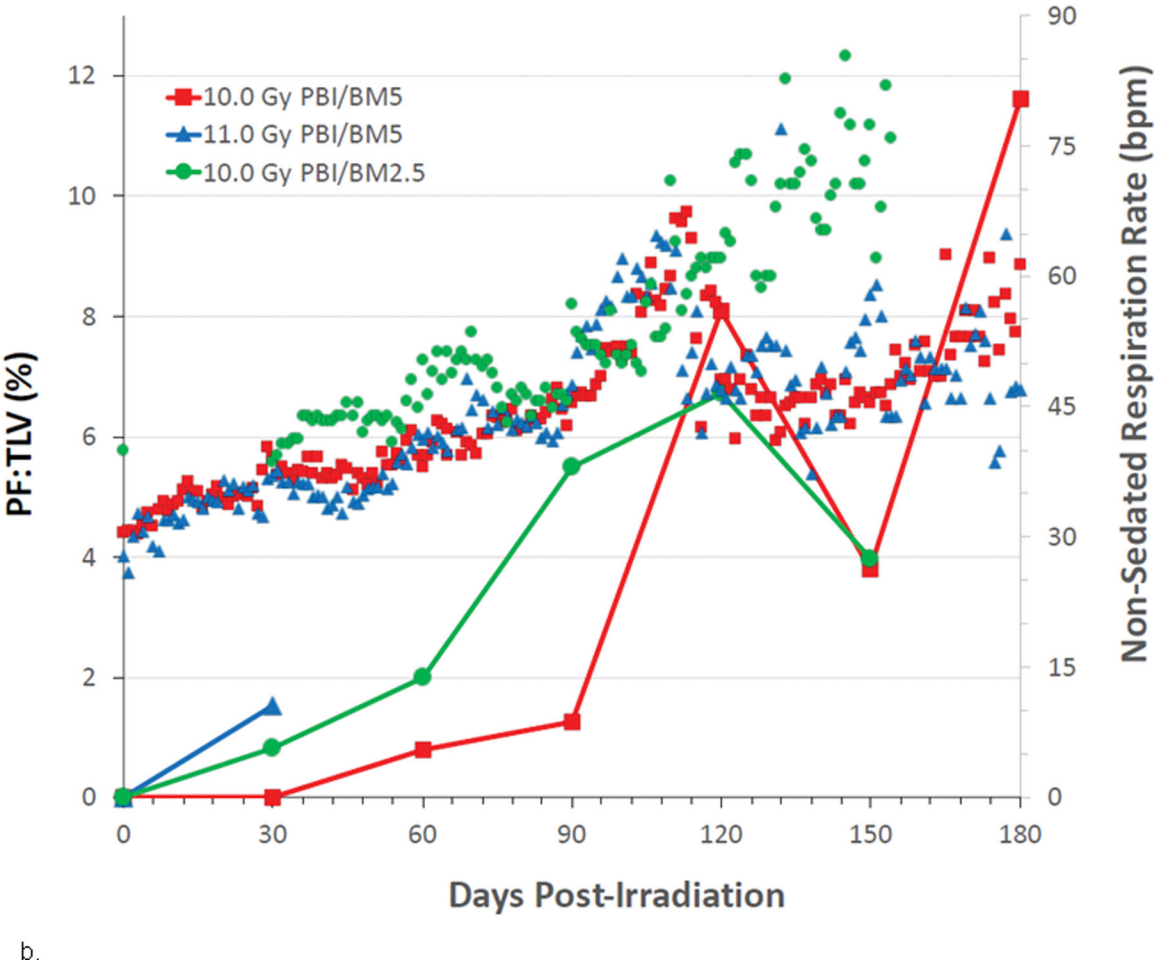

b.

Fig. 11. Comparative radiographic and clinical indices of pneumonitis/fibrosis relative to total lung volume (PF:TLV) and NSRR in NHP exposed to WTLI.

Rhesus macaques were exposed to 6 MV LINAC-derived photons delivered to prescribed dose at midline tissue (xiphoid process) at a dose rate of 0.80 Gy min^{-1} to (a) 10 to 11 Gy whole thorax lung irradiation (WTLI), or (b) 10 to 11 Gy partial body irradiation (PBI) with approximately 2.5% or 5% bone marrow (BM) sparing. Non-sedated respiratory rates (NSRR), based on the number of breaths per minute, were measured daily (scatter plots). Radiographic analysis of lung injury by computed tomography (CT), showing the mean ratio of volume of pneumonitis and fibrosis indexed against the total lung volume (PF:TLV) (solid lines) as a function of exposure dose and time post-exposure. CT scans were performed at baseline and every 30 d post-exposure until the end of study or until the animal met euthanasia criteria. Subject-based dexamethasone administration and ongoing lethality of nonhuman primates (NHP) with greatest pulmonary injury influences the results present beyond d 30 (Garofalo et al. 2014a; MacVittie et al. 2017).

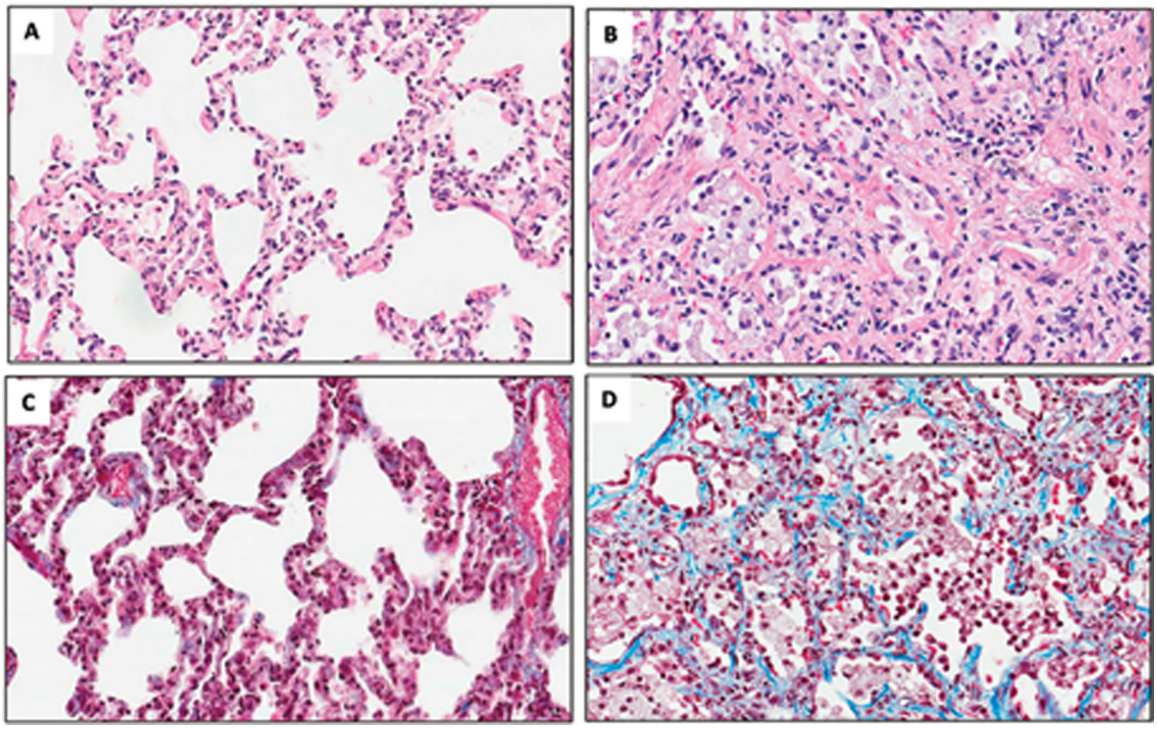

Fig. 12. Representative fields of lung tissue histology from NHP exposed to WTLI.

Representative lung tissue in a nonirradiated NHP showing normal lung morphology (A, C), and radiation-induced lung damage following 11.0 Gy whole thorax irradiation (WTLI) at 158 d post-exposure (b, d). Comparison of H&E (a, b) represent differences between a normal (a) and 11Gy irradiated (b) NHP. The irradiated NHP shows evidence of macrophage infiltration and congestion within lung architecture. Comparison of Masson's Trichrome (c, d) stains demonstrates collagen deposition consistent with fibrosis in the 11.0 Gy irradiated NHP (d) as compared with the normal NHP (c). All images are shown at 20X magnification (Garofalo et al. 2014a).

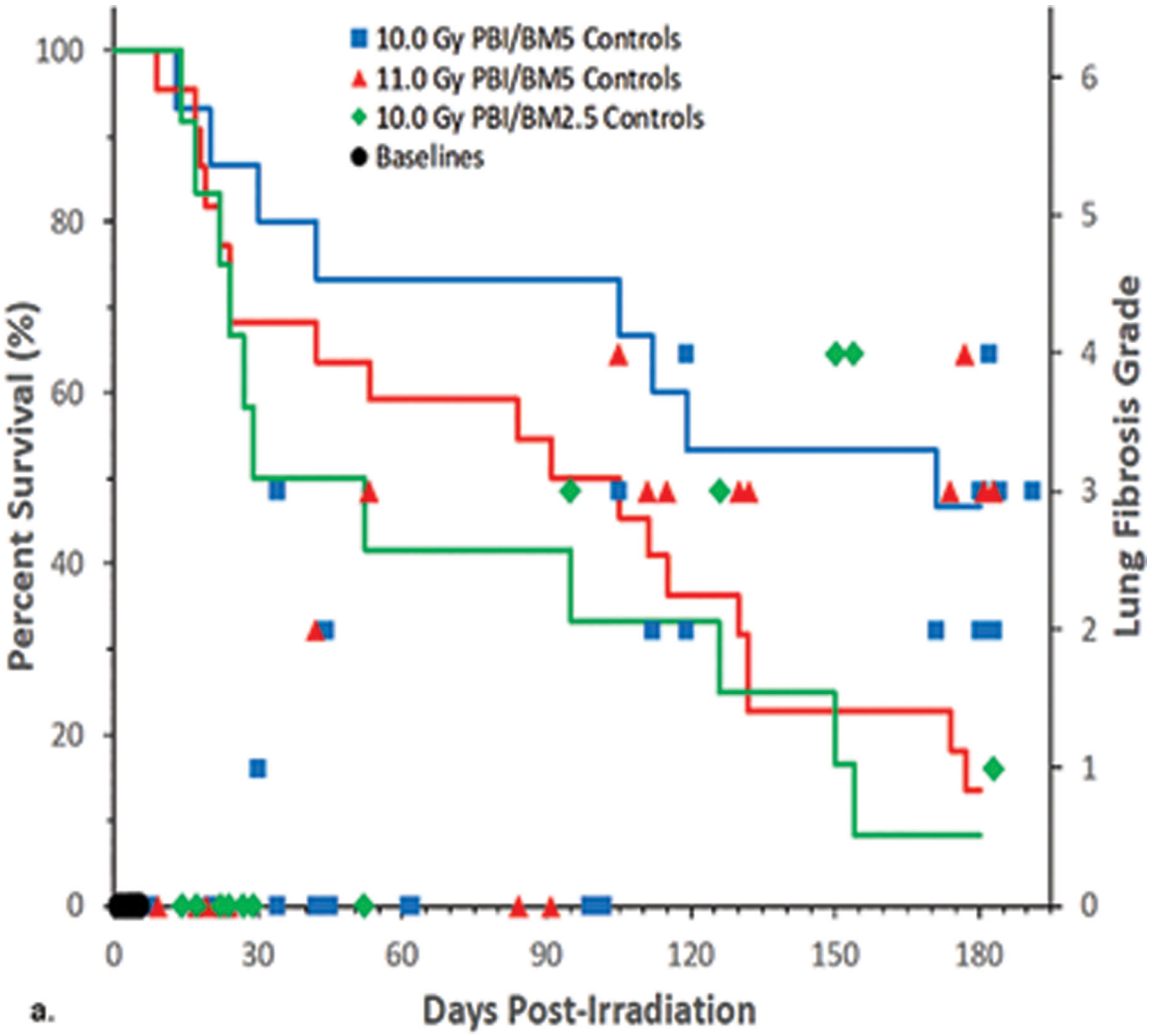

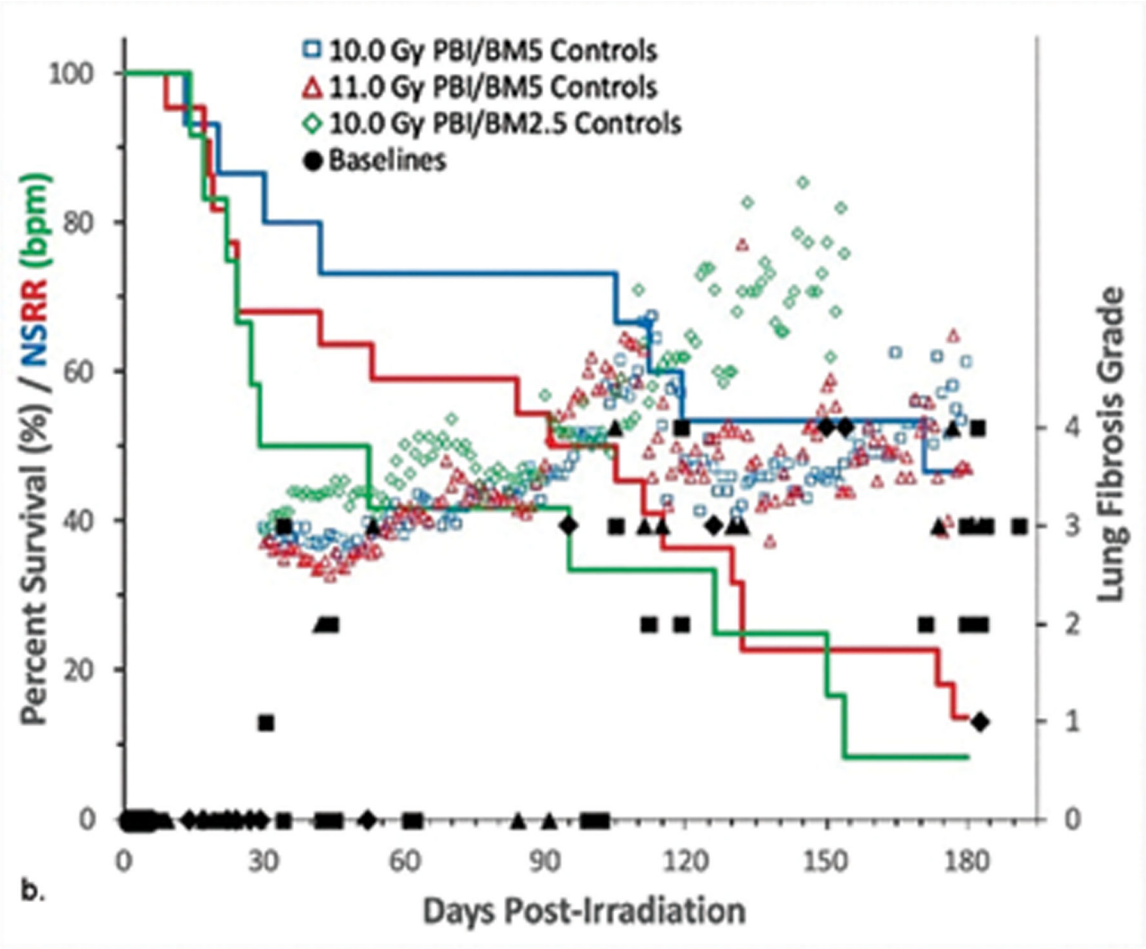

Fig. 13. Kaplan-Meier survival curves for the PBI/BM-sparing exposure protocol: Relative mortality/survival probability, histological time course of interstitial fibrosis and NSRR.

Rhesus macaques were exposed by 6 MV LINAC-derived photons delivered to prescribed dose at midline tissue (xiphoid process) at a dose rate of 0.80 Gy min^{-1} to (a) 10 or 11 Gy partial body irradiation with approximately 5% bone marrow sparing (PBI/BM5) or 10 Gy PBI/BM2.5. Animals received IACUC-approved, subject-based medical management to include dexamethasone. Lung sections were stained with Masson's trichrome to identify deposition of collagen to assess latency, incidence and severity (grade). The mean values and grade of interstitial fibrosis as a function of time (d) post exposure [(a, b) solid symbols]. There was no noteworthy difference in the incidence of interstitial fibrosis in animals irradiated at 10 versus 11 Gy. Animals were euthanized for cause throughout the 180 d study duration. Non-sedated respiratory rates (NSRR), based on the number of breaths per minute, were measured daily [(b) open symbols]. This analysis was restricted to the NHP data set that survived > 60 d post-exposure (e.g. survivors of GI-ARS and H-ARS coincident with prolonged GI and for whom serial daily NSRR data were available) (MacVittie et al. 2012; Garofalo et al. 2014a).

Table 1.

The respective LD values from the DRR for rhesus macaques exposed to PBI/BM5 or WTLI protocols.

UMSOM studies: NHP (male) were exposed to 6 MV LINAC-derived photons at a dose rate of 0.80 Gy min^{-1}, delivered at midline tissue dose (xiphoid process). The organ specific dose response relationships (DRRs) are defined by LD50 values and slopes for respective survival or all-cause mortality at 180 days post partial-body irradiation with approximately 5% bone marrow sparing (PBI/BM5) or whole thorax lung irradiation (WTLI) exposure to a range of doses in different but contemporary studies (Garofalo 2014a, MacVittie 2012, MacVittie 2017, Farese 2019) . *SNBL study*: The study performed at SNBL utilized female macaques exposed to 6 MV LINAC-derived photons at a dose rate of approximately 1.0 ± 0.05 Gy min^{-1} (Thrall 2019). All NHP received equivalent, subject-based medical management as per respective IACUC-approved criteria. Irradiations and animal care were performed at the respective radiation and veterinary facilities with the same research team in the UMSOM and that at SNBL.

Study	LD30 [Gy]	LD50 [Gy]	LD70 [Gy]	Probit Slope	n
PBI/BM5 DEARE 180 d UMSOM	9.50 [8.67,9.92]	9.94 [9.35,10.29]	10.37 [9.97,10.73]	1.21 [0.70,1.73]	87 male
WTLI DEARE 180 d UMSOM	9.78 [9.18,10.09]	10.24 [9.87,10.52]	10.70 [10.41,11.11]	1.15 [0.65,1.65]	76 male
WTLI DEARE 180 d SNBL	9.99Gy [9.45, 10.28]	10.28 [9.68, 10.92].	10.60Gy [10.32, 11.07]	1.72 [0.84, 2.60]	40 female

Table 2.

PBI/BM5 and PBI/BM2.5 Cohorts: Mortality for NHP exposed to 10 Gy or 12 Gy PBI/BM2.5 and 10 Gy, 11 Gy or 12 Gy PBI/BM5.

Rhesus macaques were exposed at 10 to 12 Gy, 6 MV LINAC-derived photons delivered to prescribed dose at midline tissue (xiphoid process) at a dose rate of 0.80 Gy min^{-1} partial-body irradiation with approximately 2.5% or 5% bone marrow sparing (PBI/BM) (MacVittie 2012, Farese 2019). Animals received IACUC-approved, subject-based medical management to include dexamethasone. The respective organ-specific and all-cause mortality [survivors/total experimental, (% mortality)] for each organ-specific time course, acute GI - ARS (1 – 15 d), H - ARS + GI damage (16 – 60 d), acute GI - ARS + H – ARS + GI damage (1 – 60 d), delayed MOI (61 – 180 d) and all-cause mortality (1 – 180 d) for 10 Gy PBI/BM2.5 or PBI/BM5.

Mortality	n	Acute GI-ARS (1–15 d)	H-ARS+ GI damage (16–60 d)	H-ARS+ GI damage (1–60 d)	Delayed MOI (61–180 d)	All Cause (1–180 d)	Survivors (180+ d)
PBI/BM5							
10 Gy	15	1/15 (7%)	3/14 (21%)	4/15 (27%)	4/11 (36%)	8/15 (53%)	7/15 (47%)
11 Gy	21	1/21 (5%)	7/20 (35%)	8/21 (38%)	9/13 (69%)	18/21 (86%)	3/21 (14%)
12 Gy	15	8/15 (53%)	------	11/15 (73%)	------	------	------
PBI/BM2.5							
10 Gy	12	1/12 (8%)	6/11 (55%)	7/12 (58%)	4/5 (80%)	11/12 (92%)	1/12 (8%)
12 Gy	22	17/22 (77%)	------	0/22 (100%)	------	------	------

Table 3.

Multiple Organ Injury (MOI): Incidence (%) of euthanasia criteria and MST (d) post-10 Gy or 11 Gy PBI/BM5 or 10 Gy PBI/BM2.5 exposure protocols in nonhuman primates.

Rhesus macaques were exposed by 6 MV LINAC-derived photons delivered to prescribed dose at midline tissue (xiphoid process) at a dose rate of 0.80 Gy min^{-1} at 10 or 11 Gy partial-body irradiation with approximately 5% bone marrow sparing (PBI/BM5) or 10 Gy PBI/BM2.5. Animals received IACUC-approved, subject-based medical management to include dexamethasone. NHP that required euthanasia due to unresolvable organ-based clinical status consequent to acute radiation syndrome are presented with the respective mean survival time (MST) (d) relative to specific euthanasia criteria.

PBI/BM5 (n = 36)	**Euthanized for cause (Incidence)**	**MST (day)**
Acute GI	5%	11
Weight Loss	16%	55
Lung Injury	19%	121
Irresolvable Edema	8%	100
H-ARS / Other Injury	16%	25
Combination of Criteria	8%	145
All-Cause Mortality	73%	77
PBI/BM2.5 (n = 12)	**Euthanized for cause (Incidence)**	**MST (day)**
Acute GI	8%	14
Weight Loss	33%	31
Lung Injury	25%	143
Irresolvable Edema	0%	NA
H-ARS / Other Injury	17%	56
Combination of Criteria	8%	29
All-Cause Mortality	92%	65

Table 4.

NSRR for NHP exposed to 10 Gy to 11.5 Gy using PBI/BM-sparing or WTLI exposure protocols, incidence and 1st day to ≥ 80 bpm.

The incidence of and latency to development of clinical pneumonitis [defined as developing a non-sedated respiration rate (NSRR > 80)] in rhesus macaques following the midplane, partial body irradiation with approximately 2.5% or 5% bone marrow sparing (PBI/BM) of 10.0 and11.0 Gy and whole thorax lung irradiation (WTLI) exposure of 10 to 11.5 Gy at UMSOM (Garofalo 2014, MacVittie 2012 and 2017, Farese 2019). WTLI was delivered at SNBL in the range of 9.9 to 11.5 Gy (Thrall 2019). Both research sites utilized 6MV LINAC-derived photons at respective dose rates of 0.80 Gy and 1.00 Gy min^{-1}. Animals received IACUC-approved, subject-based medical management to include dexamethasone. Values were recorded from NHP that survived the acute GI- and H-ARS (e.g. >60 days post PBI/BM-sparing exposure and for whom serial daily NSRR data were available). Mean latency to development of pneumonitis is shown ± the standard error of the mean.

UMSOM-PBI/BM5			**UMSOM-PBI/BM2.5**		
Dose (n)	**Incidence**	**1st day**	**Dose (n)**	**Incidence**	**1st day**
10 Gy (n = 8)	50%	127.7 ± 16	10 Gy (n = 6)	83%	98.4 ± 18
11 Gy (n = 13)	69%	98.0 ± 12			
UMSOM - WTLI			**SNBL - WTLI**		
Dose (n)	Incidence	1st day	Dose (n)	Incidence	1st day
10.0 Gy (n = 8)	63%	116.7 ± 8.0	9.5 Gy (n = 8)		131
10.5 Gy (n = 10)	70%	94.8 ± 17.7	10.0 Gy (n = 8)		114
10.74 Gy (n = 20)	85%	78.0 ± 8.0	10.5 Gy (n = 8)		82
11.0 Gy (n = 10)	90%	90.2 ± 10.6	11.0 Gy (n = 8)		80
11.5 Gy (n = 6)	100%	75.8 ± 17.6	11.5 Gy (n = 8)		58

Table 5.

Mean survival time (MST) of decedents post 10 – 12 Gy exposure using PBI/BM-sparing and WTLI protocols.

Rhesus macaques were exposed to uniform, 10.0 to 11.0 Gy partial-body irradiation with bone marrow (PBI/BM)-sparing or 10.0 to 12.0 Gy whole lung thorax irradiation (WTLI) with 6 MV LINAC-derived photons. All NHP received equivalent, subject-based medical management as per respective IACUC-approved criteria to include administration of dexamethasone. RILI and respective MST in days (d) ± standard error of the mean (SEM) of decedents, rhesus macaques (n) within the time period of 50 – 180 d post exposure are reported for each exposure cohort. PBI/BM-sparing and WTLI were conducted at UMSOM and SNBL (MacVittie, 2012; Farese 2019, Thrall 2019).

UMSOM					
PBI/BM5		**PBI/BM2.5**		**WTLI**	
Dose (n)	**MST ± SEM**	**Dose (n)**	**MST ± SEM**	**Dose (n)**	**MST ± SEM**
10 Gy (4)	126.8 ± 15.0	10 Gy (5)	115.4 ± 19.0	10.0 Gy (5)	127.8 ± 14.8
11 Gy (10)	125.1 ± 5.9			10.5 Gy (6)	114.0 ± 13.7
				10.74 Gy (15)	106.5 ± 11.7
				11.0 Gy (6)	86.2 ± 16.0
				11.5 Gy (6)	107.0 ± 17.7
				12.0 Gy (4)	89.8 ± 14.3
SNBL					
				WTLI	
				Dose (n)	MST
				10.0 Gy (6)	151.5 ± 4.9
				10.5 Gy (5)	99.6 ± 48.4
				11.0 Gy (7)	102.1 ± 31.4
				11.5 Gy (8)	81.5 ± 24.1